

A Cause of Sudden Acceleration in Battery Powered Electric Vehicles – Rev 3

by

Ronald A. Belt
Plymouth, MN 55447
27 January 2023

Abstract: A cause of sudden acceleration in a generic class of battery-powered electric vehicles (BeV's) is discussed. The cause is associated with the voltage compensation algorithm used in all such vehicles to correct the motor operating point for changes in DC link voltage that accompany changes in the state of charge (SOC) of the high voltage battery. Normally this battery voltage compensation causes an increase in the motor speed of 25% or less. But when the battery voltage is sensed during a negative voltage spike caused by the inrush current of an electric motor turning on, then an incorrect DC link voltage reading results that causes the standard compensation algorithm to increase the motor speed by over 300x. This condition persists until another DC link voltage reading is taken many minutes later. In the meantime, the motor operating point associated with a released accelerator pedal is suddenly increased to an operating point in the field weakening region. If the motor stator voltage then exceeds the incorrectly sensed DC link voltage of the high voltage battery, then an unstable condition exists in the control electronics in which control of the motor operating point is lost. The motor torque can then increase without control, resulting in sudden unintended acceleration without the driver pressing on the accelerator pedal.

This revision analyses two different controller designs to determine how they behave when an error occurs in the DC link voltage. In both cases sudden unintended acceleration can occur in both the driver-controlled mode and the autopilot mode without the driver's foot being on the accelerator pedal. In both cases and both designs, sudden acceleration can occur randomly when a negative-going voltage spike occurs at the time the DC link voltage sensor is digitized, which may coincide with some motor turning on, such as a power steering boost motor, a power brake booster motor, a stability control pressure pump motor, or an HVAC pump motor. And in both cases and both designs, the sudden acceleration mode can disappear completely when the DC link voltage sensor is digitized again without a voltage spike being present, leaving no trace of hardware fault, software fault, or diagnostic trouble code (DTC). However, the accelerator pedal sensor reading in the EDR behaves differently in the two designs. In the first design it will not be changed during faulty controller operation unless the driver presses on the accelerator pedal because it is likely derived from a signal that appears earlier in the controller chain of operations, such as before or after the pedal map. In the second design it is possible for it to increase without the driver's foot being on the accelerator pedal during faulty controller operation because it is likely derived from a signal after the signal has been changed by the faulty controller operation. One can determine which controller design applies in a given situation by performing a dynamometer test to check how the torque behaves with changes in the SOC of the high voltage battery. If the torque changes with battery SOC, then the first controller design applies. If it does not change with battery SOC, then the second controller design applies. These results show that it is important to analyze any different controller design in a similar fashion to determine how it behaves during faulty controller operation.

Introduction

This paper discusses a cause of sudden acceleration in a generic class of battery-powered electric vehicles (BeV's) having similar design features. By discussing the operation of a generic class of vehicles, design features that cause sudden acceleration can be discussed without naming any

specific vehicle manufacturer or any specific vehicle model in the paper. This guarantees that the paper will not cause financial damage to any specific vehicle manufacturer that might elicit a cease and desist order demanding removal of the paper from publication under threat of being sued for damages to the manufacturer's reputation and stock price. Such an order can be used by vehicle manufacturers to eliminate discussion of potential defects in their vehicles while claiming that their vehicles have no such design defects and while benefitting from media articles from friendly authors and postings from friendly users that blame the driver for sudden acceleration.

The class of vehicles to be discussed in this paper has the design features listed below. These features can be found in vehicles from multiple vehicle manufacturers, avoiding the implication that they narrow the class to a single vehicle manufacturer. This suggests that sudden acceleration in BeV's is an industry-wide problem, and not just a problem for a single vehicle manufacturer.

Control system features of vehicles in this class:

- 1) Two or more pedal position sensors are used to convert the driver's depression of the accelerator pedal into a voltage input to the vehicle control system.
- 2) A pedal map converts the accelerator pedal position sensor output into a motor torque request.
- 3) An inverse motor map converts the motor torque request into (i_d^* , i_q^*) current commands or (torque*, flux*) commands needed to operate the motor at the desired torque and speed.
- 4) Field oriented control (FOC) algorithms are used to control the motor (i_d , i_q) currents to the reference (i_d^* , i_q^*) or (torque*, flux*) commands.
- 5) Motor control algorithms vary with the motor speed region.
- 6) Vehicles with multiple electric motors use a torque distribution system between the pedal map and the inverse motor map to distribute the total vehicle torque as needed between front and back electric motors as well as between left and right rear motors if used.

Electric drive motor features of vehicles in this class:

- 1) Drive motors consist of interior permanent magnet synchronous motors (IPMSM). Other motor types such as induction motors (IM) or surface permanent magnet synchronous motors (SPMSM) are also possible, but are used less often.
- 2) Torque dependence on speed varies with motor speed region.
- 3) Torque depends only on motor current in the region below base speed.
- 4) Field weakening is required when operating the motor above base speed.
- 5) Voltage limiting is required when operating the motor at the highest speeds.
- 6) Motor operated in regen mode provides negative torque to slow the vehicle.
- 7) Slowing down with regen instead of brake recharges battery and increases driving range
- 8) Regen torque provides deceleration levels of about 0.2 to 0.3 G.
- 9) Regen allows one pedal driving.
- 10) One or more electric motors are used per vehicle.
- 11) Some vehicles in this class control regen with the brake pedal instead of the accelerator pedal. This changes regen operation, but does not change the motor control features.
- 12) Exception not included in this class:
 - a) Hybrid vehicles add an internal combustion engine to either recharge the battery or to apply torque in parallel or in series with the electric motor.

A Cause of Sudden Acceleration In Battery Powered Electric Vehicles – Rev 3

- 1) Vehicle battery consists of:
 - a) Modules internally wired as a parallel combination of strings of battery cells with multiple cells in each string wired in series.
 - b) Cells strung in series within a module provide a module voltage of about 40V to 50V that is intermediate between the cell voltage and the full battery voltage.
 - c) Parallel strings within a module provide a much higher module current than a single cell.
 - d) Modules in series provide the desired vehicle battery voltage and current.
- 2) Vehicles have a similar high voltage DC battery voltage of 400V maximum or 360V average. A battery voltage of 800V maximum is also possible in this class, but its use is limited by the availability of components having a higher breakdown voltage.
- 3) Battery voltage varies with battery state of charge (SOC).
- 4) Vehicles have a similar battery voltage range of 300V to 400V for the 400V battery.
- 5) An inverter powered by the DC battery bus provides three-phase AC voltages to the motor's stator windings while regulating the motor's torque by varying the stator currents.
- 6) An electric power steering motor draws power from the 12V battery bus
- 7) Exceptions not included in this class:
 - a) Some eV's use a DC/DC converter between the battery and the drive motor

I. Control System Operation for This Generic Class of BeV's

Figure 1 shows a block diagram of the control system design used in this generic class of vehicles. This block diagram was created from information obtained from multiple academic technical papers and theses dealing with electric motor control. [1,2,3,4,5,6,7,8] It was not obtained from any vehicle manufacturer. It is assumed, however, that this block diagram applies to all the vehicles of this class of BeV's because the control of electric motors in these vehicles has the same fundamental motor control issues as the control of electric motors used in a host of other industries. Therefore, there is a rich technical open literature dealing with electric motor control design and operation that applies to this widespread need for control.

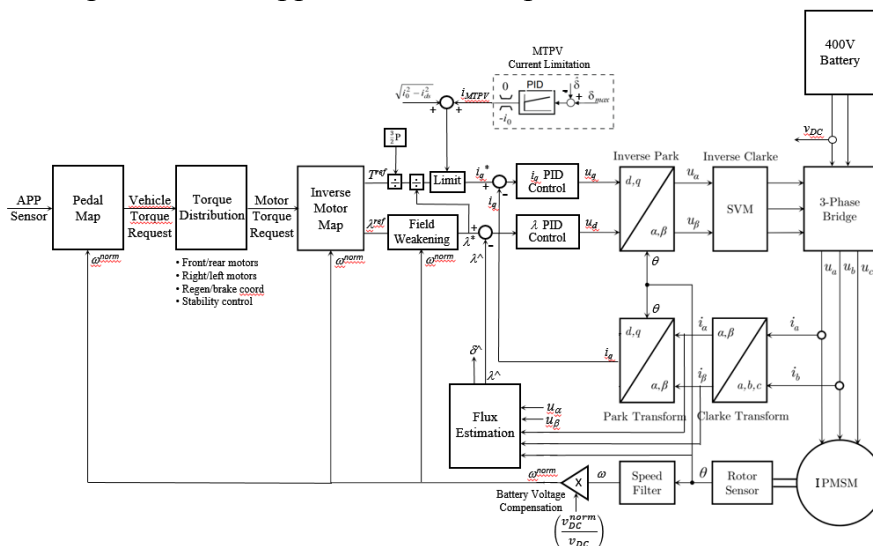


Figure 1. Block diagram of the control system of a typical vehicle in this class of BeV's. This diagram uses (torque, flux) reference coordinates. An alternate diagram using (i_d^* , i_q^*) reference coordinates is shown in Appendix A.

In Figure 1, two or more accelerator pedal position (APP) sensors are used to convert the driver's depression of the accelerator pedal into a voltage input to a pedal map. The pedal map, which is usually a look-up table, then generates a vehicle torque request based on the APP sensor input and the current vehicle speed. The vehicle torque request is then distributed across the front and rear motors of the vehicle, and possibly the right and left motors, as needed for proper motor efficiency, proper braking, and stability control until it becomes a motor torque request for each individual electric motor. The motor torque request and motor speed then become the inputs into an inverse motor map that supplies as outputs the required (torque, flux) values or (i_d , i_q) motor currents needed for the motor to achieve the desired motor torque and motor speed used as inputs¹. The inverse motor map is usually a look-up table whose outputs become the reference inputs or set-points for the PID controllers that control the currents within the electric motor. The PID controllers then compare the actual (torque, flux) values or (i_d , i_q) currents within the electric motor to the reference (torque*, flux*) or (i_d^* , i_q^*) set-points supplied by the inverse motor map to control the (torque, flux) values or (i_d , i_q) currents in the motor by driving the difference between the two PID inputs to zero. By using a field-oriented control (FOC) control scheme as shown in the blocks to the right of the PID controllers, these PID controllers can operate at a DC level in the fixed laboratory frame even as the currents in the electric motor vary in magnitude and phase in a rotating frame fixed to the motor's rotor. The FOC control blocks are carried out using high-speed digital computations that convert the DC current values in the fixed laboratory frame to stator current values in the rotating current frame and then back again to the fixed frame. The conversion between the fixed and rotating frames is done by using forward and inverse Park transformations while forward and inverse Clark transformations convert two orthogonal coordinates into three-phase stator drive coordinates and back again. The physical conversion into stator currents is done indirectly by turning on and off high voltage drive transistors in a DC to AC inverter that pulse width modulates the current drawn from a high voltage DC link into three-phase currents applied to the motor stator windings. Current and voltage sensors on the stator terminals then provide the phase currents and voltages that are sent back to the PID controllers to provide proper control.

The content of the inverse motor map is shown in Figure 2. The inverse motor map is a table that contains the reference (torque*, flux*) commands or (i_d^* , i_q^*) PID set-points for each of the motor operating points falling below the maximum torque versus motor speed curve shown in Figure 2. The driver determines the torque value of any of these operating points, and the vehicle speed automatically determines the motor speed. As the vehicle speed changes, the motor operating points follow a curve in the torque/speed plane. A similar map in the torque/speed plane but mirrored across the motor speed axis has negative torque values that determine the regen level at which the motor operates while slowing down.

¹ The term "inverse motor map" comes from the observation that the physical motor converts current inputs into torque and speed outputs. Therefore, the inverse operation to the physical motor corresponds to supplying torque and speed as inputs to a map that supplies the motor currents as outputs. Clearly, the inverse motor map operation must be a true mathematical inverse of the original motor operation, or else the control system will have defects.

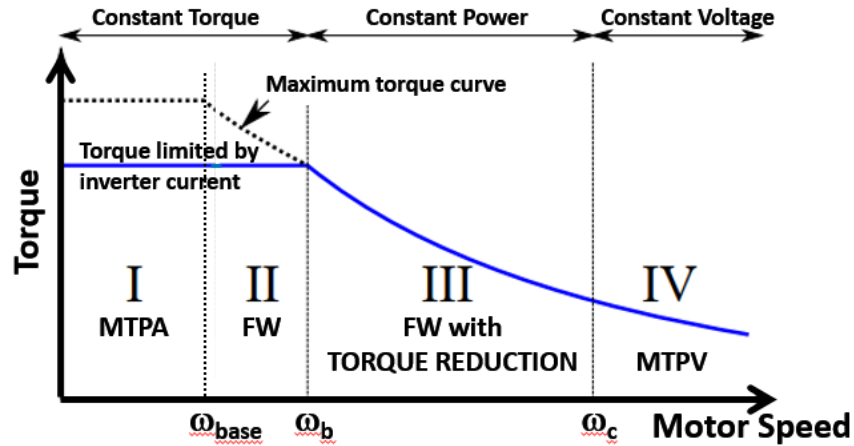


Figure 2. The inverse motor map is a table that contains the reference (torque*, flux*) values or (i_d^* , i_q^*) set-points for each of the motor operating points falling below the maximum torque versus motor speed curve shown in the figure.

Motor torque varies differently with motor speed in each of the four sub-regions of this table. In region I the motor torque is determined only by the motor current, which can be limited either by the maximum inverter current or by the maximum motor power. The motor operating points in this region are usually calculated to provide the maximum torque per ampere (MTPA) of current in order to obtain the most efficient use of the battery. As the motor speed increases in Region I, the back EMF of the motor increases until it becomes equal to the DC battery voltage at a speed known as the base speed, ω_{base} . Operation of the motor above base speed then becomes impossible without limiting the EMF by field weakening. As the motor speed increases, this field weakening causes the maximum motor torque to decrease inversely with the motor speed as shown in Region III. If the motor torque is not limited by the inverter current, then this field weakening Region III begins at the base speed. But if the maximum motor torque is limited to a lower torque value by the maximum inverter current, then the maximum torque can remain constant for a while in a Region II before torque reduction is needed. As the motor speed increases with field weakening, a speed is reached at which further field weakening to reduce the back EMF voltage is impossible. Operation above this speed in Region IV of the table requires voltage limiting in addition to field weakening. This causes the maximum torque to decrease inversely with the square of motor speed in Region IV. In Region IV the operating points are usually calculated to provide the maximum torque per volt (MTPV) of applied voltage.

The existence of these four speed ranges explains the inclusion of the field weakening block in Figure 1 as well as the MTPV circuitry shown in the figure. Further details explaining how the algorithms carry out these functions will not be discussed at this time. The flux estimation block is needed to compute a flux value from the sensed stator currents and voltages that can be used in the feedback to the PID controller that sets the flux value for the motor. Flux estimation algorithms vary with motor speed because some algorithms become unstable at low motor speeds while others become unstable at high motor speeds. Often a weighted sum of algorithms is used with the weighting factors changing with motor speed.

Figure 2 shows that the boundaries of the four speed ranges of the inverse motor map depend upon the value of the back EMF voltage relative to the DC battery voltage. This means that different algorithms must be used in each speed range to calculate the motor operating points at the proper DC battery voltage. The look-up table used for this map usually assumes that the battery voltage used for this calculation is the maximum DC voltage of the high voltage battery.

For this class of vehicles this voltage is usually 400 volts. Since the table values remain fixed, this voltage value remains fixed also.

Now, it is well known that that DC voltage of a high voltage battery varies with the state of charge (SOC) of the battery. Figures 3 and 4 show how much this voltage varies with the state of charge. For the two different battery chemistries shown, the DC battery voltage decreases from about 400V to 300V as the battery state of charge decreases from 100% to about 10%. This implies a voltage drop of about 25%. This size of a voltage drop will have a noticeable effect on electric motor performance unless something is done to compensate for it.

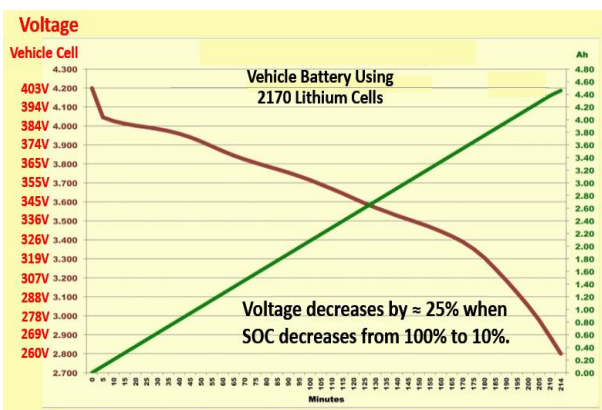


Fig 3. Voltage versus state of charge (SOC) for a lithium battery using 2170 type cells.

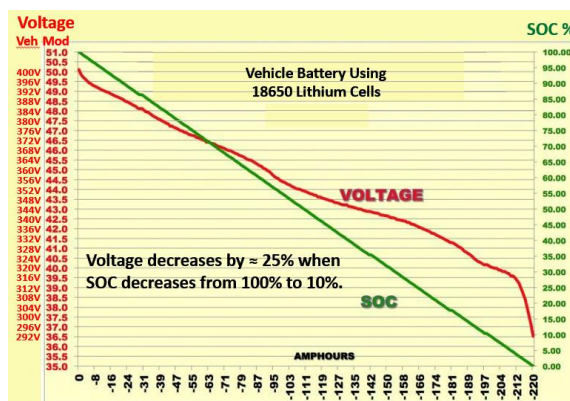


Fig 4. Voltage versus state of charge (SOC) for a lithium battery using 18650 type cells.

Figure 5 shows what happens when the torque and power of vehicles in this class are measured during a dynamometer test in which the state of charge (SOC) of the high voltage battery is varied between tests. One finds that as the battery state of charge decreases, the torque curves shift to the left to lower motor speeds while the maximum torque remains constant for all SOC values. A decrease in the battery state of charge from 100% to 10% causes the torque curve to shift to a lower speed that is about 25% lower.

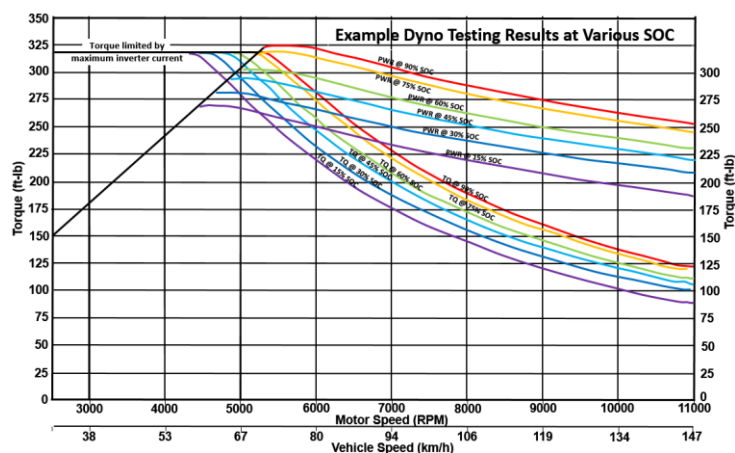


Figure 5. Dynamometer testing^[9] shows that the vehicle torque and power curves shift to lower motor speeds as the state of charge of the high voltage battery decreases. The maximum torque for all curves remains constant because it is limited by the inverter current.

Figure 6 shows what this same data would look like if the maximum motor torque is limited by the high voltage battery instead of by the inverter current. In this case the torque values above the inverter current limit become visible. They show that the speed changes in the torque curves

result from changes in the battery voltage associated with the changing SOC values. As the SOC values decrease the battery voltage decreases, causing the field weakening region to shift to lower motor speeds. This causes the motor base speed to shift to lower motor speeds. A decrease in the SOC from 100% to 10% causes a decrease in battery voltage from 400V to 300V, or about 25%. This causes a shift in the motor speed of about 25%.

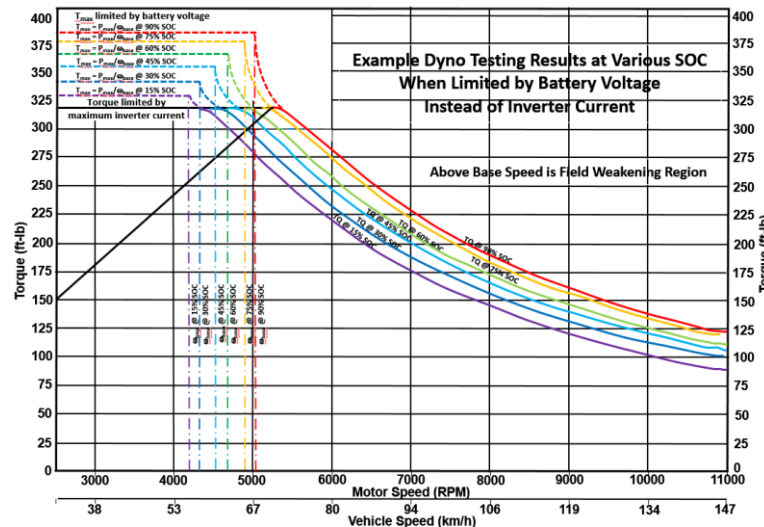


Figure 6. If the torque curves in Figure 5 were limited by battery voltage instead of inverter current, then the same data would look like this, showing that the speed shifts in the torque curves are caused by battery voltage changing as a result of SOC changes.

So how does the motor control system deal with these changes in the maximum torque curve with SOC when the inverse motor map is a look-up table that has a single fixed maximum torque curve with four different regions that are defined relative to a fixed battery voltage of 400V? The answer is shown in Figure 7. Figure 7 shows that as the battery voltage decreases to cause the torque curves to shift to the left, the control system senses the DC battery voltage and shifts the curves back to the right by the inverse ratio of the battery voltages, causing each curve to realign with the curve in the inverse motor map. This correction results in a maximum increase in the motor speed of about 25% that offsets the maximum decrease in motor speed of about 25% caused by a battery voltage shift of 25% associated with a maximum change of SOC value from 100% to 0%. This so-called battery voltage compensation is shown in the lower right hand corner of the control system block diagram shown in Figure 1 above.

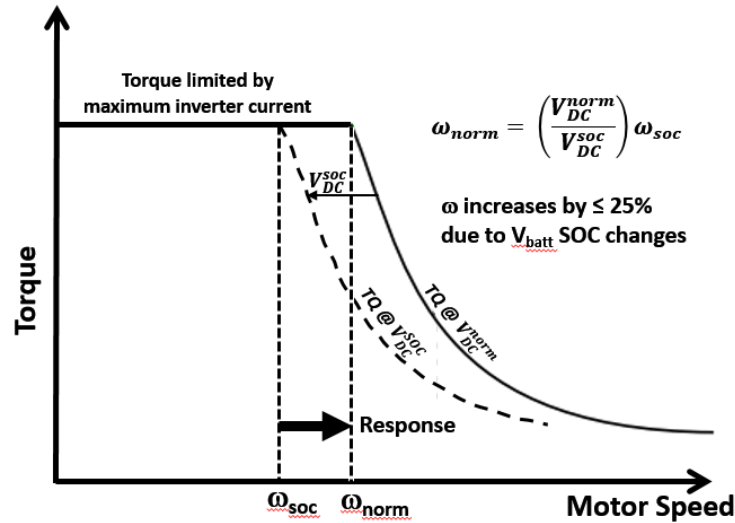


Figure 7. When the battery voltage decreases from the normal 400V value with decreasing SOC, causing the torque curve to shift to a lower motor speed, the control system senses the battery voltage and multiplies the motor speed by the inverse ratio of battery voltages to bring the torque curve back to its original 400V value. This is called battery voltage compensation.

Figure 8 shows what happens to the operating points in the inverse motor map when battery voltage compensation is applied. The operating point associated with the lower battery voltage is shifted to the right to a higher motor speed by the voltage compensation value to cause a different operating point to be selected whose torque/speed value corrects for the lower battery voltage that is currently active. This shifts all operating points by the same compensation value. In particular, the operating point associated with a released accelerator pedal² is shifted by this compensation value, which results in a shift in motor speed of about 25% maximum as the SOC changes from 100% to 0%. This causes the motor operating point of the released accelerator pedal to remain in the MTPA region where the torque depends only on the motor current. The result is only a small change in the motor speed and no change in the motor torque. This means the battery voltage compensation corrects exactly for the changes in battery voltage with SOC, allowing the motor to operate normally at all times. This is exactly how the control system is expected to work as designed.

² The inverse motor map often specifies a small positive torque at the lowest motor speeds in order to give the vehicle a small speed that mimics creep in an internal combustion vehicle with an automatic transmission. Sometimes this creep function can be turned on and off by the driver, but sometimes the positive torque remains present even when the creep function is turned off.

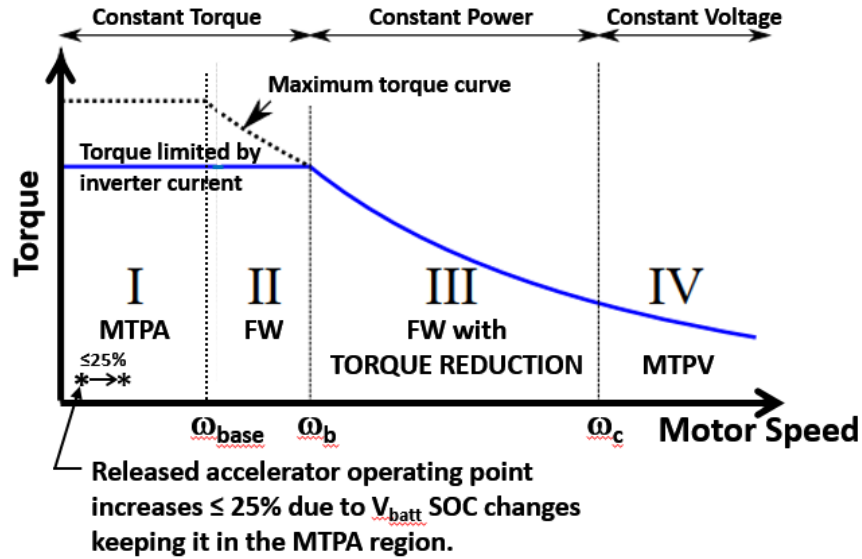


Figure 8. Battery voltage compensation causes a shift in the motor operating point within the inverse motor map as the battery voltage changes with decreasing SOC. This shift in motor operating point is normally a maximum of 25% in speed, which causes the motor operating point of the released accelerator pedal to remain in the MTPA region where the torque depends only on the motor current. This produces no change in the motor torque.

II. Control System Operation With Voltage Spikes

While the control system works correctly under normal circumstances for all vehicles in this class, a condition unexpected by many designers can cause improper operation in some vehicles. This unexpected condition is the presence of negative-going voltage spikes on the output of the DC link voltage sensor. These negative-going voltage spikes cannot be present on the DC link itself because of the large capacitance of several hundred farads placed on this link to keep the RMS voltage variations below a specified amount. Therefore, the negative-going voltage spikes must originate somewhere else in the system and then find their way into the output of the DC link voltage sensor.

Figure 9 shows a block diagram of the electronic power system found in this class of BeV's. It shows that the DC link voltage sensor is actually common to two power busses; namely, the high voltage DC link and the 12V battery supply bus. Therefore, these negative-going voltage spikes may be produced on the 12V battery supply bus. They are likely to be produced by the function that draws the most current, which is the electric power steering function that draws over 100 amps peak at times during normal operation. The negative-going voltage spikes are produced by the inrush current of the electric power steering motor when it turns on.³ This happens because the motor windings are essentially a wire that causes a direct short to ground when the motor is first turned on until a magnetic field can build up in the motor to limit the current through the windings. This temporary short to ground causes an extremely high current through the motor that pulls the 12V DC bus voltage down from 12V or less to near zero volts until a magnetic field builds up in the motor to limit the current. At this time the 12V supply

³ The power steering motor turns on only when a torque assist is needed to help the driver turn the front wheels while a load is being placed on the steering mechanism that makes it harder to turn. This can happen when a driver turns the steering wheel at low speed when the friction between the front tires and the road becomes greater as the speed decreases. This condition is found most often when turning into a perpendicular parking space while slowing the vehicle to a stop. This condition happens to be the same condition that leads to a majority of sudden acceleration incidents.

voltage increases back to its original value of 12.6V or less. This field buildup may take several hundreds of microseconds to occur, during which a negative voltage spike is created on the 12V DC supply bus.

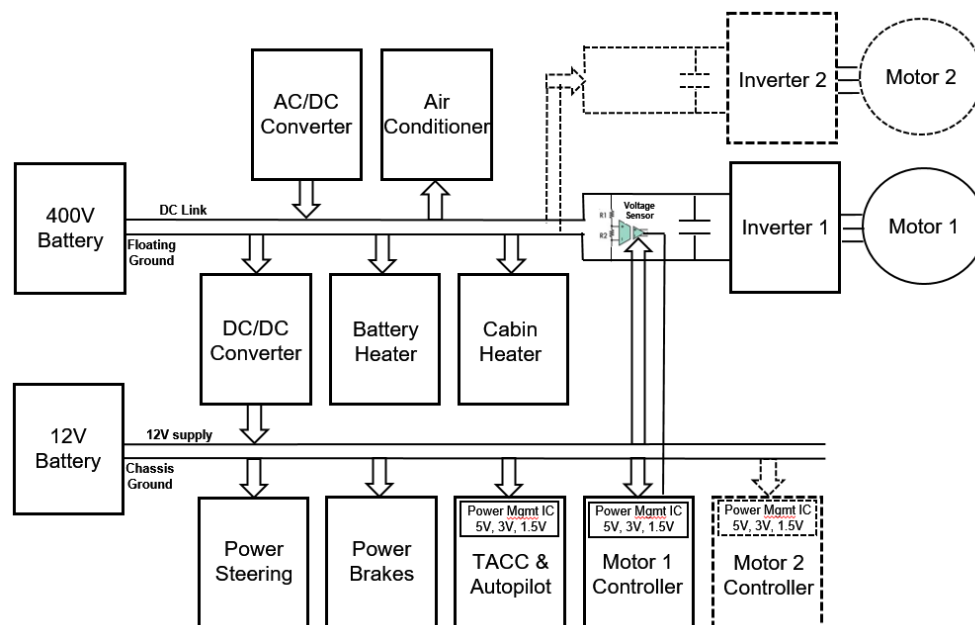


Figure 9. Block diagram of the power system in battery-powered eV's of this class. The DC link voltage sensor is common to both the high voltage DC link and the 12V battery supply bus. Therefore, negative-going voltage spikes on the output of this sensor can originate in the 12V supply bus instead of the DC link, which has a very high capacitance on it that prevents negative-going voltage spikes.

To understand how these negative-going voltage spikes get into the output of the DC link voltage sensor, it helps to know how such sensors operate. Figure 10 and Figure 11 show two types of isolated voltage sensors, a simple inexpensive type having a maximum temperature of 105°C and a more robust and more expensive type having a much higher temperature range. It is not known which type is used by vehicles in this class of eV's. But both types of sensors have similar features. Both sensors have a high voltage section and a low voltage section separated by a high voltage dielectric. The two sections communicate across the dielectric either by using an analog IR LED signal or a digital modulator signal. This not only allows different voltage levels to be used in each section, but it also maintains a floating ground in the high voltage section while providing a normal chassis ground in the low voltage section. The high voltage section is powered by the high voltage being measured, which in this case 400V. It is connected to the DC link by means of a two resistors forming a voltage divider. It draws only a few milliamps, so it's practically invisible to the battery and the inverter on the DC link. The low voltage section is usually powered by a regulated 5V supply found in a power management integrated circuit located on one of the motor controller boards. The 5V output of the voltage sensor is then divided down to a voltage level of about 3V that is compatible with the A/D converter in the DSP found on the same board that is used to control the motor.

We can now explain how the negative-going voltage spikes produced on the 12V battery bus get into the output of the DC link high voltage sensor. First, they pass from the 12V battery bus to the 5V regulator in the power management integrated circuit. They do this when the power management IC senses that a negative-going voltage spike is present on the 12V battery bus, at which time it goes into reset, causing the 5V regulator to turn off. When the power management

IC comes out of reset, the 5V regulator turns back on again. This interruption in the 5V regulator output within the power management IC causes an interruption in the sensor bias of the DC link voltage sensor that produces a negative-going voltage spike on the sensor output. The voltage spike has a voltage of zero volts and a duration equal to the duration of the reset in the power management IC, which is a just few tens of microseconds longer than the original negative-going voltage spike on the 12V supply bus. An interesting feature of the power management IC, however, is that the 3V regulator to the A/D converter and the 1.5V regulator to the digital part of the DSP do not turn off during the reset of the power management IC.⁴ Therefore, the A/D converter can continue to operate and digitize the output of the DC link voltage sensor that now has a negative voltage spike on it.

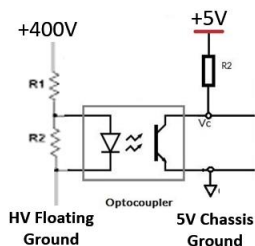


Fig 10. Simple inexpensive voltage sensor good to 105°C

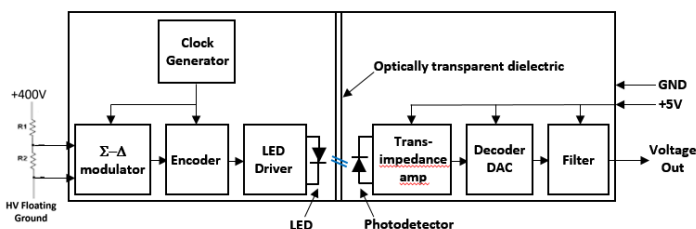


Fig 11. More robust and more expensive voltage sensor for temperatures above 105°C

Even though there may be negative voltage spikes on the output of the DC link high voltage sensor, the A/D converter may not always see them. Figure 12 shows how this can happen. In Figure 12 the top trace shows that the voltage on the DC link usually falls in the gray area within 25% of the maximum battery voltage of 400V. There are no spikes on this DC link voltage.

The second trace shows that negative-going voltage spikes can exist on the 12V battery bus that have a voltage close to zero volts. These spikes occur randomly and have a duration of several hundred microseconds. They are caused by the inrush current of an electric motor turning on, which is usually the electric power steering motor that has an extremely high current capability.

The third trace shows that these negative-going spikes get transferred to the 5V power supply when the 5V power supply is reset during a voltage spike on the 12V power bus. The spikes on the 5V power supply then get transferred to the output of the DC link high voltage sensor when the 5V bias supply turns off and then back on again.

The lowest trace shows what happens when the output of the DC link voltage sensor is digitized by an analog-to-digital (A/D) converter with and without any negative-going voltage spikes. The trace shows that the A/D converter has a sample time of only 10 microseconds or so, which is an extremely short duration. These samples are also taken at a very low rate, on the order of one sample every few minutes or so, because the DC link voltage doesn't change very rapidly. Therefore, most of the time when the A/D samples the DC link voltage, the correct DC link voltage is obtained. However, once in a very great while, as the A/D converter sample is being taken, a negative-going voltage spike randomly occurs. This causes the A/D converter to digitize the extremely low voltage of the voltage spike, which is near zero volts, instead of the true DC link voltage of the high voltage battery. The probability of this happening is a random event having a very low probability because the durations of the negative-going spike (~ 200 us) and

⁴ This is likely to allow the DSP to keep providing PWM commands to the SiC power transistors in the inverter to prevent the back EMF of the motor from blowing the power transistors if they shut off while the vehicle is moving at high speed.

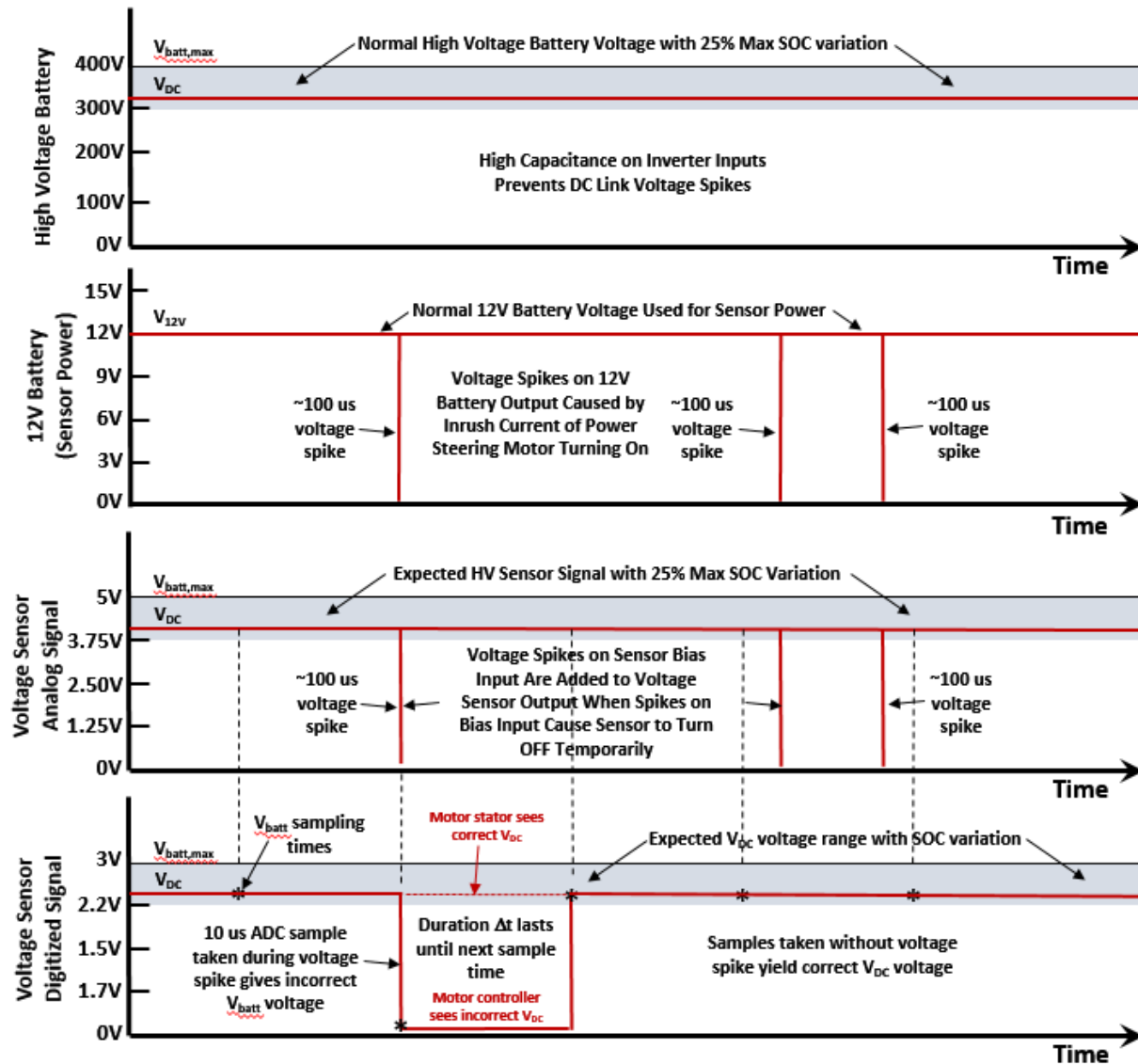


Figure 12. The high voltage DC battery voltage usually falls in the gray area within 25% of the maximum battery voltage of 400V. There are no spikes on this DC link voltage. But random negative-going voltage spikes on the 12V battery bus can have a voltage close to zero volts. These spikes get transferred to the 5V power supply when the 5V power supply is reset during a voltage spike on the 12V power bus and then to the output of the high voltage DC voltage sensor through its 5V bias supply. When the A/D samples the output of the high voltage DC battery voltage sensor with these spikes, most of the time the correct DC battery voltage is obtained. But if the A/D converter samples the output of the high voltage DC voltage sensor during a negative voltage spike, then the motor controller sees an incorrect voltage close to zero volts. Meanwhile, the voltage seen by the motor stator remains at the correct DC battery voltage of 300V to 400V. This discrepancy in voltages lasts until the next A/D sample is taken, and has an adverse effect on control system performance.

the A/D sample time (~10 us) are extremely small while the times between the A/D samples and between the negative-going voltage spikes are orders of magnitude larger (~minutes). Nevertheless, such a random coincidence of A/D sampling and spike duration is possible and it determines the incident rate for sudden acceleration in this class of vehicles.⁵

The bottom trace also shows that once an incorrect DC link voltage is obtained by this random process, the incorrect DC link voltage lasts until the next A/D sample, which can be several minutes later. In the meantime, the voltage that the stator of the electric motor sees remains at the true DC link voltage value of between 300V to 400V while the voltage that the control system sees is the incorrectly digitized A/D value of approximately 0V. This large discrepancy in voltage values has an adverse effect on the control system operation. Yet, after a new A/D sample is taken, this large discrepancy in voltage values is no longer present, and the control system behaves normally again as though nothing happened. This ability to “heal” afterward explains the inability to find a vehicle defect after a sudden acceleration incident. In fact, not only does the control system operate correctly in this case both before and after the voltage discrepancy, but also during the discrepancy. It is merely a temporary change in the voltage environment that causes the adverse effect on the control system, and not a defect in the control system itself. But this incorrect voltage can be avoided by testing the sampled voltage immediately after sampling and then sampling again if the voltage is abnormally low. This could prevent any adverse effects from happening.

So what adverse effect does the incorrect high voltage DC battery voltage obtained by the A/D converter have on control system operation? Table 1 shows that this incorrect battery voltage causes the torque vs. motor speed curve to shift to an extremely low motor speed on the order of a few RPM.

Table 1. The extremely low voltage obtained by the A/D converter during a negative voltage spike causes the torque vs motor speed curve to shift to an extremely low motor speed on the order of a few RPM. In contrast, the smaller voltage changes associated with SOC reduction produce a $\leq 25\%$ change in motor speed.

V_{batt}	SOC	ω_e
400V	100%	5200 RPM
390V	90%	5050 RPM
375V	75%	4900 RPM
355V	60%	4650 RPM
335V	45%	4500 RPM
315V	30%	4300 RPM
300V	15%	4200 RPM
3V	(0%)	42 RPM
1V	(0%)	14 RPM

When this happens, Figure 13 shows that the battery voltage compensation algorithm then increases the motor speed by the inverse amount of 300x to 400X. Figure 14 shows how this affects the motor operating point selected in the inverse motor map. In this case the battery voltage compensation causes a shift in the motor operating point within the inverse motor map in response to an incorrect battery voltage obtained during a negative voltage spike. The shift in motor operating point causes a 300x to 400x increase in motor speed, which causes the motor operating point of the released accelerator pedal to shift into the field weakening region with torque reduction. This causes the control system to apply a field weakening algorithm to the

⁵ It should be possible to calculate the random rate of occurrence of a coincidence between an A/D sample and a negative-going voltage spike from the data given. This has not been done yet.

operating point that looks at the stator voltage with respect to the DC battery voltage. If the stator voltage exceeds the DC battery voltage, then the operating point lies in an unstable region in which the control system loses control of the motor torque.

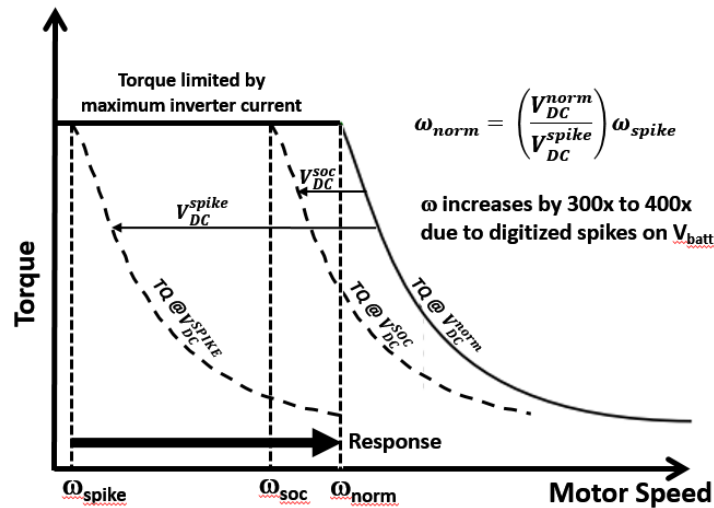


Figure 13. The extremely low incorrect battery voltage obtained by an A/D converter during a negative voltage spike causes the torque vs. voltage curve to shift to a motor speed value close to zero RPM. The battery voltage compensation algorithm then shifts it back to a higher value by the inverse amount of 300x to 400x.

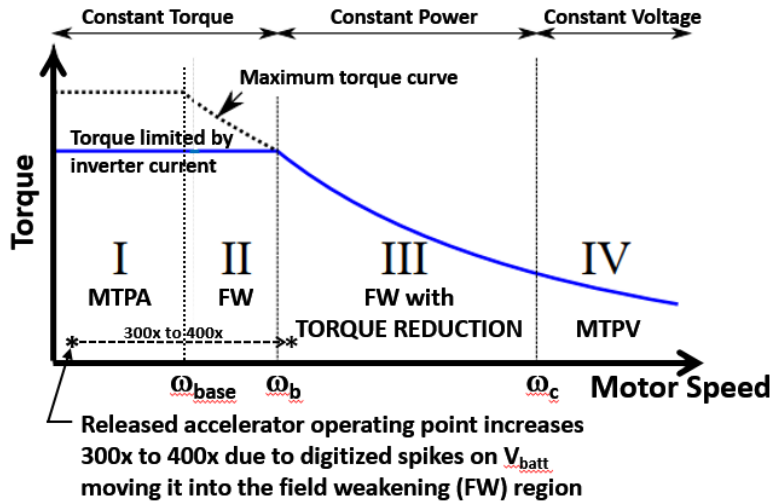


Figure 14. Battery voltage compensation causes a shift in the motor operating point within the inverse motor map in response to an incorrect battery voltage obtained during a negative voltage spike. The shift in motor operating point caused by a voltage spike is between a 300x to 400x increase in motor speed, which causes the motor operating point of the released accelerator pedal to shift into the field weakening region with torque reduction. This causes the control system to apply a field weakening algorithm to the operating point that looks at the stator voltage with respect to the DC battery voltage. If the stator voltage exceeds the DC battery voltage, then the control system is in an unstable region in which it loses control of the motor torque.

Simulation results obtained by a team of academic researchers [10,11,12] show that if the stator voltage exceeds the DC battery voltage, then the operating point lies in an unstable region in which the control system loses control of the motor torque. Figure 15 shows the LUT-based FOC motor control scheme they simulated along with battery voltage compensation to correct the shift in the torque curve caused by SOC reduction in a high voltage battery voltage. Their simulation included a VCT block that could be excluded to show how the present battery voltage compensation scheme can lead to unstable operation or added to show how their proposed VCT scheme prevents unstable operation.

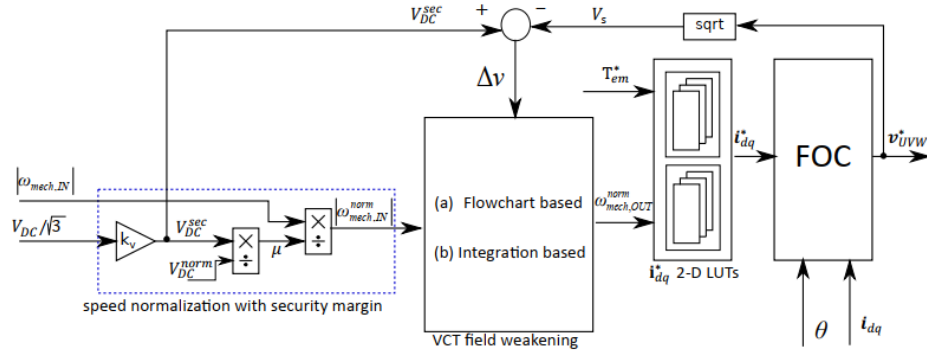


Figure 15. A LUT-based FOC motor control scheme was simulated that used battery voltage compensation to correct the shift in the torque curve caused by SOC reduction in a high voltage battery voltage.[10,11,12] The VCT block could be excluded to determine whether the normal battery voltage compensation scheme could lead to unstable operation or added to show how a proposed VCT scheme could prevent such unstable operation.

Figure 16 shows the results they obtained. For these simulations the battery voltage was changed only a small amount from its normal value as typical of normal SOC variations, so large variations caused by voltage spikes were not assumed. Figure 16 shows that even with normal changes in the voltage of the high voltage battery with SOC changes, one can encounter unstable operation in the field weakening region if the stator voltage exceeds the battery voltage. This unstable operation allows the motor torque to increase without limit as shown in Figure 16.

A similar situation can exist when a negative voltage spike causes the digitized battery voltage to be sensed as being lower than the stator voltage when the motor operating point is set at a low motor speed while the accelerator pedal is either not being pressed by the driver or while it is being pressed only a very small amount. The former situation can happen when the vehicle has a small positive motor torque that simulates creep in a conventional vehicle with an internal combustion engine and an automatic transmission. In these cases the motor torque is not increased if the motor operating point stays in Region I because the motor torque is a function of motor current in this region. But if the battery voltage compensation algorithm translates the motor speed to a much higher speed, the motor operation enters into field weakening region III, where the field weakening algorithm compares the stator voltage to the voltage of the high voltage battery. If it then finds that the stator voltage exceeds the voltage of the high voltage battery, then the algorithm determines that the motor is in an unstable region and loses control of the torque. The torque can then increase without limit, causing sudden acceleration.

The loss of motor control during sudden acceleration is further enhanced by a dynamic effect in which the voltage controller in the field weakening control loop can't keep up with a rapid change in the sensed battery voltage. This is discussed further in Appendix C.

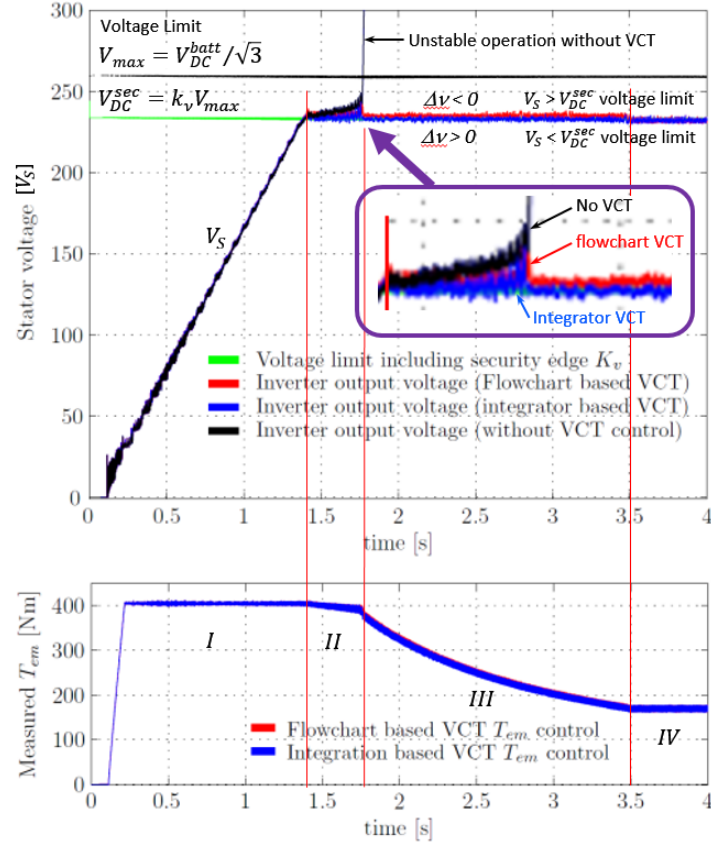


Figure 16. Simulation results ^[10,11,12] show that as the motor operating point increases along the maximum torque curve, the stator voltage increases with increasing motor speed. As the motor speed passes through the field weakening region II, with the present battery voltage compensation scheme the torque begins to increase when it shouldn't because the stator voltage exceeds the secure voltage of about 240V. As the speed enters into field weakening region III, when the stator voltage exceeds the battery voltage, control becomes unstable leading to the torque increasing without limit (black trace above). The proposed VCT algorithm prevents such unstable operation (red and blue traces above) .

Figure 17 shows a proposed flowchart-based voltage constraint algorithm for avoiding the instability caused by the stator voltage being higher than the voltage of the high voltage battery^[10,11,12]. And Figure 18 shows a proposed integration-based voltage constraint algorithm having the same objective ^[10,11,12]. The algorithms work by adjusting the motor speed either higher or lower to keep the stator voltage below a secure voltage level that is slightly below the voltage of the high voltage battery. The data in Figure 16 show that both of these algorithms work as expected, with the integration-based algorithm being slightly better than the flowchart-based algorithm. Figure 19 shows how either of these two algorithms fit into the block diagram of a complete motor control system.

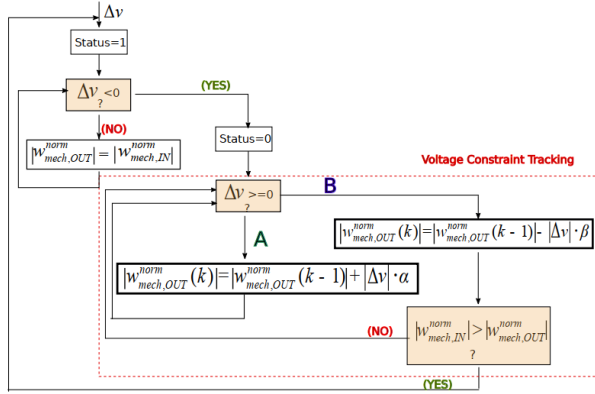


Fig 17. Proposed flowchart-based voltage constraint tracking (VCT) algorithm^[10,11,12]

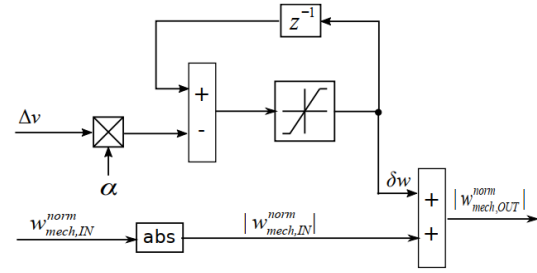


Fig 18. Proposed integration-based voltage constraint tracking (VCT) algorithm^[10,11,12]

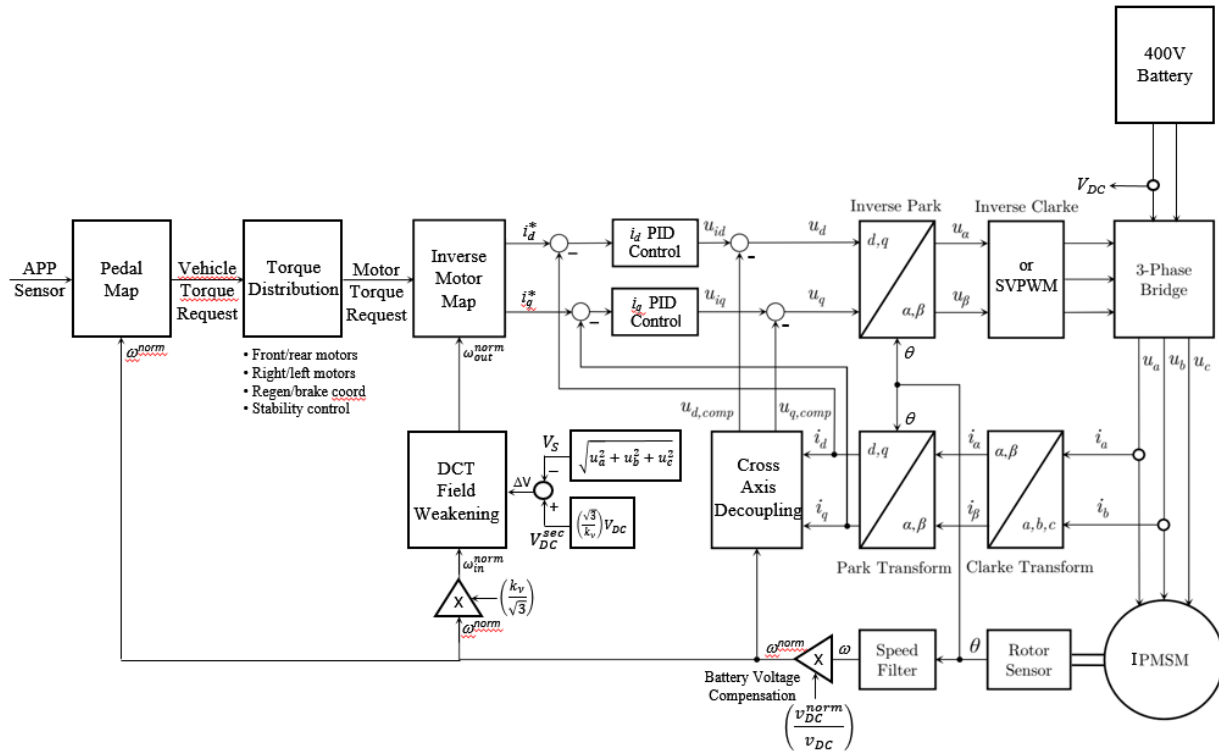


Figure 19. Block diagram of a complete FOC-based motor control system using a voltage constraint tracking algorithm for field weakening that can prevent loss of torque control when the stator voltage exceeds the voltage of the high voltage battery. Field weakening is included in the inverse motor map, but only when the DC link voltage is at a maximum. The DCT field weakening block extends field weakening to other DC link voltages.

III. Operation When The Requested Torque Is Below the Maximum Value

The preceding sections have considered only the case when the motor speed changes with the state of charge (SOC) of the high voltage battery. In this case we found that a decrease in the SOC of the high voltage battery causes a decrease in the battery voltage that translates into a decrease in the DC link voltage powering the drive motors. A decrease in the SOC from 100% to 10% causes a decrease in the DC link voltage of about 25%, which causes a decrease in the motor's base speed of up to 25%. This means that the motor's base speed calculated from the

motor's stator voltage and current outputs can be up to 25% less than the motor's base speed assumed when the torque and flux set-points are issued by the inverse motor map, which assumes a motor base speed associated with the $V_{\text{DCLink}}(\text{MAX})$. Therefore, in order to achieve proper control of the motor at a lower SOC value, the measured base speed of the motor must be multiplied by the ratio of $V_{\text{DCLink}}(\text{MAX})/V_{\text{DCLink}}(\text{SOC})$ before using it as an input to the inverse motor map. This works well under most circumstances. But when there is an error in the sensed value of $V_{\text{DCLink}}(\text{SOC})$ causing it to be much lower than the normal minimum value of $V_{\text{DCLink}}(\text{SOC})$, then the ratio $V_{\text{DCLink}}(\text{MAX})/V_{\text{DCLink}}(\text{SOC})$ becomes > 100 times greater than the normal ratio of 1 to 1.33. This can cause the controller to operate in the field weakening region while the motor is still operating in the base region. This can result in unstable operation in the field weakening region as discussed in the previous section, which can lead to sudden unintended acceleration.

We will now consider the case of how the motor torque is changed when there is an error in the sensed value of $V_{\text{DCLink}}(\text{SOC})$ causing it to be much lower than the normal minimum value of $V_{\text{DCLink}}(\text{SOC})$. To do this, we will consider two possible controller designs. In the first controller design the maximum torque in the base region is limited by the inverter current, while the maximum torque in the field weakening region can still decrease with battery SOC. This first controller design is found to allow sudden acceleration to occur in both the driver mode and the autopilot mode while the accelerator pedal sensor reading in the EDR remains unaffected. In the second controller design the maximum torque is not limited by the maximum current. Instead, the PWM duty cycle applied to obtain a desired torque value is increased by the ratio $V_{\text{DCLink}}(\text{MAX})/V_{\text{DCLink}}(\text{SOC})$ that neutralizes the decrease in the torque with SOC. This causes the maximum torque in both the base region and the field weakening region to remain unchanged as battery SOC decreases. This second controller design is found to allow sudden unintended acceleration to occur in both the driver mode and the autopilot mode while the accelerator pedal sensor reading in the EDR is also increased without the driver's foot being on the accelerator pedal. These two cases show that the controller design can have a critical impact on the effects of sudden unintended acceleration even when the same mechanism is the cause of sudden unintended acceleration. Therefore, it is important to analyze any new controller design in a fashion similar to how the designs in this section are analyzed.

A. Motor and controller with the maximum torque in the base region limited by the maximum current.

What we expect to see with normal operation in this case is summarized in Figure 20. The back EMF of the motor increases linearly with motor speed until it reaches the DC link voltage at a speed known as the base speed. The motor cannot go any faster than the base speed unless the controller prevents the BEMF from increasing further by weakening the stator flux in proportion to the increasing motor speed. This separates motor operation into a base region and a field weakening region. In the base region the maximum torque T_{MAX} is proportional to the product of the stator flux Ψ_s and the maximum current I_{MAX} , both of which are independent of motor speed. I_{MAX} is limited by the maximum current that the inverter can provide to a value below which the torque cannot decrease further as the DC link voltage decreases with battery SOC. In the field weakening region the flux and maximum torque vary inversely with motor speed and decrease as the DC link voltage decreases with battery SOC. All torques less than these maximum torques are obtained by PWM modulation of the maximum torques and have the same dependence on DC link voltage as the maximum torques.

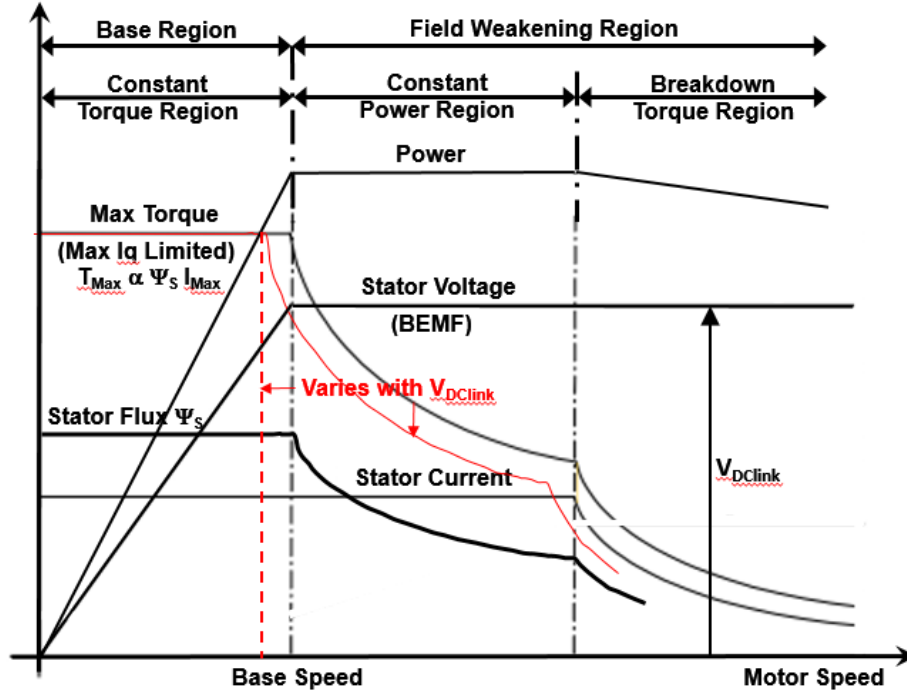


Figure 20. The back EMF of the motor increases linearly with motor speed until it reaches the DC link voltage at a speed known as the base speed. The motor cannot go any faster than the base speed unless the controller prevents the BEMF from increasing further by weakening the stator flux in proportion to the increasing motor speed. This separates motor operation into a base region and a field weakening region. In the base region the maximum torque T_{MAX} is proportional to the product of the stator flux Ψ_s and the maximum current I_{MAX} , both of which are independent of motor speed. I_{MAX} is limited by the maximum current that the inverter can provide to a value below which the torque cannot decrease further as the DC link voltage decreases with battery SOC. In the field weakening region the flux and maximum torque vary inversely with motor speed and decrease as the DC link voltage decreases with battery SOC. All torques less than these maximum torques obtained by PWM modulation of the maximum torques have the same dependence on DC link voltage as the maximum torques.

We now assume that the controller uses flux-torque variables like the block diagram shown in Figure 21. With this block diagram in mind, we can analyze how the motor controller carries out its operations. These operations are shown in Table 2. Table 2 assumes that both the motor and the controller are operating normally with the same V_{DCLink} value.

First, the controller uses the measured motor speed as an input to the inverse motor map. To do so, it must multiply the motor speed by the ratio $[V_{DCLink(max)}/ V_{DCLink(SOC)}]$ to correct for the motor speed varying with $V_{DCLink(SOC)}$ while the contents of the motor map are calculated using an assumed value of $V_{DCLink(max)}$. If the corrected motor speed falls in the base region of the map, then the operations shown in the left-hand column of Table 2 are performed. If the corrected motor speed falls in the field weakening region of the map, then the operations shown in the right-hand column of Table 2 are performed. In the base region the controller operations cause the motor flux and maximum torque to remain constant with ω and V_{DCLink} , with the maximum torque being limited by the maximum inverter current. In the field weakening region the controller operations cause the flux and maximum torque to vary inversely with motor speed and to decrease as the V_{DCLink} voltage decreases. Torques less than the maximum torque are obtained by PWM modulation of the maximum torque and have the same dependence on DC

The diagram illustrates the control architecture for a 400V battery-powered IPMSM. The system components and their interconnections are as follows:

- 400V Battery:** Provides the DC link voltage V_{DC} to the 3-Phase Bridge.
- 3-Phase Bridge:** Converts the DC link voltage into three-phase AC voltages u_a, u_b, u_c for the IPMSM.
- IPMSM:** Represented by the equation $T = \frac{3}{2} p \lambda i_t$, where T is torque, p is the number of pole pairs, λ is the flux linkage, and i_t is the torque current.
- Rotor Sensor:** Provides the rotor position θ to the Park and Clarke transforms.
- Speed Filter:** Filters the rotor position signal to provide a smooth speed ω .
- Flux Estimation:** Estimates the flux linkage λ based on the motor's electrical parameters and the measured currents.
- Clarke Transform:** Converts the three-phase currents i_a, i_b, i_c into the d, q frame currents i_d, i_q .
- Park Transform:** Converts the d, q frame currents i_d, i_q into the α, β frame currents i_α, i_β .
- Inverse Park:** Converts the α, β frame currents i_α, i_β back into the d, q frame currents i_d, i_q .
- Inverse Clarke:** Converts the d, q frame currents i_d, i_q back into the three-phase currents i_a, i_b, i_c .
- Inverse Motor Map:** Converts the torque request T_{ref} into the torque current i_t^* .
- Motor Torque Request:** Provides the torque reference T_{ref} to the Inverse Motor Map.
- Torque Distribution:** Distributes the torque request among the three phases.
- Vehicle Torque Request:** Provides the torque reference T_{ref} to the Torque Distribution block.
- Pedal Map:** Provides the torque reference T_{ref} to the Vehicle Torque Request block.
- APP Sensor:** Provides the torque reference T_{ref} to the Pedal Map block.
- Control Loop:** The torque current i_t^* is compared with the measured torque current i_t to generate a current error. This error is processed by a PID controller to produce the d -axis current reference i_d^* . The d -axis current reference i_d^* is then compared with the measured d -axis current i_d to generate a current error. This error is processed by a PID controller to produce the d -axis voltage reference u_d^* . The d -axis voltage reference u_d^* is then compared with the measured d -axis voltage u_d to generate a voltage error. This error is processed by a PID controller to produce the d -axis current reference i_d^* . The d -axis current reference i_d^* is then compared with the measured d -axis current i_d to generate a current error. This error is processed by a PID controller to produce the d -axis voltage reference u_d^* . The d -axis voltage reference u_d^* is then compared with the measured d -axis voltage u_d to generate a voltage error. This error is processed by a PID controller to produce the d -axis current reference i_d^* .

A Cause of Sudden Acceleration In Battery Powered Electric Vehicles – Rev 3

Table 2. Summary of motor behavior and combined motor controller operations when both are operating normally with the same V_{DCLink} . The controller first determines the region in which the motor is operating and then sets the flux and maximum torque accordingly. In the base region the flux and maximum torque are held constant and the maximum torque is limited by the maximum inverter current. In the field weakening region the flux and maximum torque vary inversely with motor speed and decrease as V_{DCLink} decreases. Torques less than the maximum torque are obtained by PWM modulation of the maximum torque and have the same dependence on DC link voltage as the maximum torques. The result is shown by the experimental dynamometer results in Figure 22.

	Base Region	Field Weakening Region
Motor Behavior Only	1) If $BEMF \leq V_{DCLink}$, \Rightarrow base region 2) $BEMF = \text{constant} \times \omega_M$ 3) $T = \text{const} \times \Psi_{PM} I_q$ 4) T is independent of ω_M 5) T decreases as V_{DCLink} decreases.	1) If $BEMF > V_{DCLink}$, then motor is inoperable.
Assumes V_{DCLink} is the same for both motor and controller		
Combined Motor and Controller Operation	1) Calculate $[V_{DCLink}(\text{max})/V_{DCLink}(\text{SOC})]$. 2) If $\omega \times [V_{DCLink}(\text{max})/V_{DCLink}(\text{SOC})] < \omega_{\text{base}}$, then the motor is operating in the base region. 3) Set the λ^* set-point equal to the λ^{ref} output of the inverse motor map to keep the flux constant with ω and V_{DCLink} in the base region 4) Set the i_t^* set-point equal to T^{ref}/λ^* to keep the torque constant with ω and V_{DCLink} in the base region. 5) The i_t^{\wedge} and λ^{\wedge} feedback values from the motor should not vary with ω and V_{DCLink} , just as the set-points i_t^* and λ^* do not vary with ω and V_{DCLink} 6) The base speed ω_{base} should decrease with V_{DCLink} 7) The measured motor flux and torque should not vary with ω or V_{DCLink} in the base region	1) Calculate $[V_{DCLink}(\text{max})/V_{DCLink}(\text{SOC})]$. 2) If $\omega \times [V_{DCLink}(\text{max})/V_{DCLink}(\text{SOC})] > \omega_{\text{base}}$, then the motor is operating in the field weakening region 3) Apply field weakening to the the λ^{ref} output of the inverse motor map to obtain the λ^* set-point, making the flux vary with ω and V_{DCLink} in the FW region. 4) Set the i_t^* set-point equal to T^{ref}/λ^* to make the torque vary with ω and V_{DCLink} in the FW region. 5) The i_t^{\wedge} and λ^{\wedge} feedback values from the motor should vary with V_{DCLink} in the same fashion as the set-points i_t^* and λ^* 6) The base speed ω_{base} should decrease with V_{DCLink} 7) The measured motor flux and torque should vary with ω and V_{DCLink} in the FW region

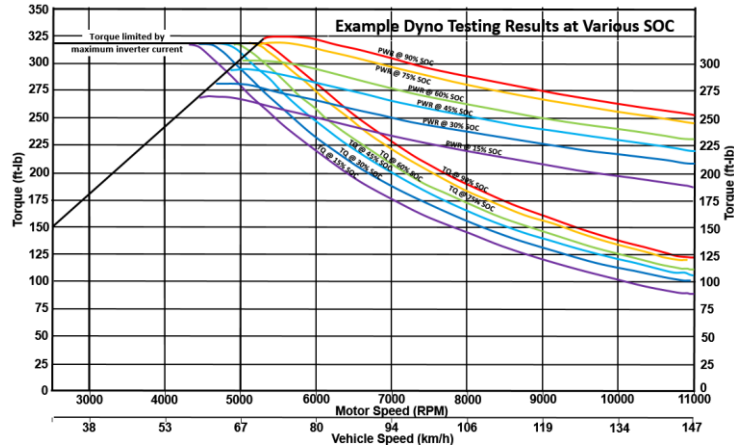


Figure 22. Dynamometer testing⁶ shows that the maximum torque and power curves shift to lower motor speeds as the state of charge (SOC) of the high voltage battery decreases. This implies that the base speed shifts to lower motor speeds as the DC link voltage decreases and that the torque in the field weakening region decreases with decreasing DC link voltage.

The maximum torque below base speed remains constant because the motor current is limited by the inverter to create a maximum torque that is independent of the DC link voltage varying with the SOC of the high voltage battery. All lower torques derived from these two maximum torques by PWM modulation have the same dependence on DC link voltage as the maximum torques.

We now consider what can happen if there is an error in the sensed DC link voltage caused by a negative-going voltage spike making the sensor output temporarily lower while it is being digitized by an A to D converter. Section II discusses how this error can occur. This error can make the normal voltage $V_{DCLink}(SOC)$, which varies by about 25% from a voltage $V_{DCLink}(max)$ of 400V, change to a faulty voltage $V_{DCLink}(faulty)$ which is close to zero volts, or a change of greater than 100 times. To make the error even worse, this large voltage change only affects the controller, while the motor continues to operate at the voltage $V_{DCLink}(SOC)$, which is 100 times higher.

Figure 23 shows what can happen to the torque/speed curve when this error occurs. The decrease in motor speed caused by the decrease in DC link voltage from $V_{DCLink}(SOC)$ to $V_{DCLink}(spike)$ makes the controller believe that the base speed has decreased by the ratio $V_{DCLink}(spike)/V_{DCLink}(SOC)$ from ω_{soc} to ω_{spike} . Meanwhile, the motor continues to operate at the base speed of ω_{soc} . Therefore, the controller concludes incorrectly that the motor is operating in the field weakening region when the motor continues to operate in the base region. This causes the controller to apply field weakening operations to the motor while operating in the base region, which produces a faulty operation of the controller.

⁶ Dynamometer test results courtesy of Mountain Pass Performance located in Toronto, Canada.

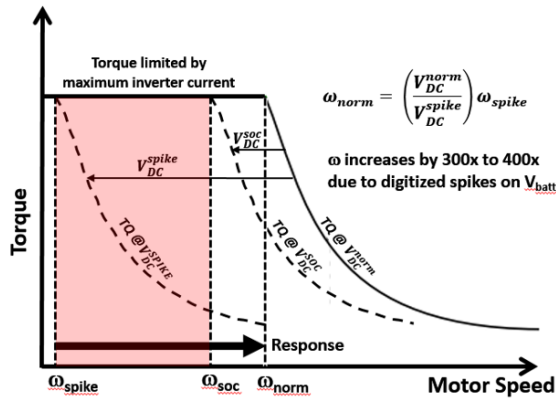


Figure 23. If the controller determines the base speed is at ω_{spike} while the motor continues to operate at the base speed ω_{soc} , then the controller concludes incorrectly that the motor is operating in the pink field weakening region when the motor continues to operate in the base region. This creates an incompatibility between the controller set-points and the feedback signals from the motor which causes the controller to become unstable.

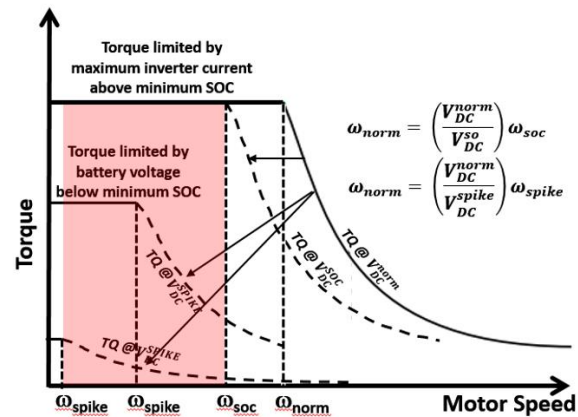


Figure 24. It is believed that the torque in the base region may also decrease when the base speed decreases from its minimum SOC value ω_{soc} to ω_{spike} based on the argument in Figure 25. But a decrease in torque has no effect on the change in base speed from ω_{soc} to ω_{spike} . So the analysis of controller operations for this case is the same as for the case in Figure 23.

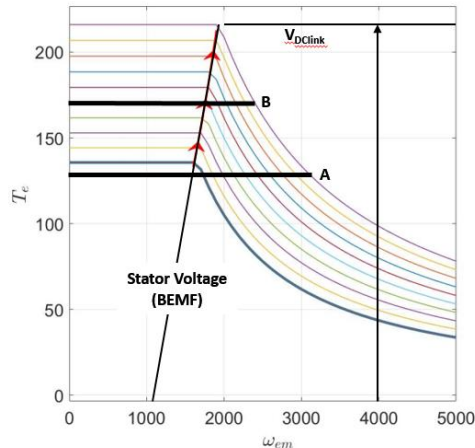


Figure 25. If the maximum torque is set at level A below the torque associated with the minimum value of $V_{\text{DCLink}}(\text{SOC})$, then all torques obtained from this maximum torque by PWM modulation are independent of the $V_{\text{DCLink}}(\text{SOC})$ voltage. But if the maximum torque is set at a level B such that some torques at values of $V_{\text{DCLink}}(\text{SOC})$ are above it and some are below it, then torques below it will still vary with $V_{\text{DCLink}}(\text{SOC})$ voltage, and all torques obtained from these torques below level B by PWM modulation will depend on the $V_{\text{DCLink}}(\text{SOC})$ voltage below level B. This will also happen when $V_{\text{DCLink}}(\text{SOC})$ changes to $V_{\text{DCLink}}(\text{faulty})$, where $V_{\text{DCLink}}(\text{faulty})$ is much less than the minimum $V_{\text{DCLink}}(\text{SOC})$ value.

We can now analyze how the motor controller behaves when the DC link voltage V_{DCLink} changes to $V_{\text{DCLink}}(\text{faulty})$ while the motor is operating in the base region. In this case, operations using $V_{\text{DCLink}}(\text{faulty})$ are performed on the combined motor/controller outputs in the base region with the motor still at the $V_{\text{DCLink}}(\text{SOC})$ value. These operations are shown in Table 3.

First, the controller adjusts the measured motor speed by the ratio $V_{\text{DCLink}}(\text{max})/V_{\text{DCLink}}(\text{faulty})$ and then uses it as an input to the inverse motor map. If the adjusted motor speed falls in the base region of the map, then the operations shown in the left-hand column of Table 3 are performed. In the faulty base region the controller operations cause the motor flux and maximum torque to remain constant with ω and V_{DCLink} , with the maximum torque being limited by the maximum inverter current. These are the same operations that one would expect to use when the motor is operating in its true base region. So no changes are produced by operating the controller with the lower DC link voltage $V_{\text{DCLink}}(\text{faulty})$.

If the corrected motor speed falls in the field weakening region of the map, then the operations shown in the right-hand column of Table 3 are performed. In this case the controller performs the field weakening operations shown using the DC link value $V_{\text{DCLink}}(\text{faulty})$ while the motor is still operating in the base region with the DC link value $V_{\text{DCLink}}(\text{SOC})$. This causes the λ^* and i_t^* set-points to have very low values associated with $V_{\text{DCLink}}(\text{faulty})$ while the feedback values i_t^{\wedge} and λ^{\wedge} from the motor will have higher values associated with $V_{\text{DCLink}}(\text{SOC})$. In this case, the feedback values to the PID controllers are over 100x greater than the set-point values, causing the PID controllers to have negative inputs. Therefore, the PID controllers begin to operate without negative feedback, allowing the PID outputs to increase without bound. This can cause sudden unintended acceleration even if the driver has not stepped on the accelerator pedal.

Since the fault in this case occurs in the FOC controller, faulty operation leading to sudden acceleration can occur either in the driver-controlled mode or in the autopilot mode of vehicle operation. In either mode of operation, sudden acceleration can occur without the driver's foot being on the accelerator pedal. Also, in either mode of operation, sudden acceleration can occur randomly when a negative-going voltage spike happens to occur at the time the DC link voltage sensor is digitized, which may coincide with some motor turning on, such as a power steering boost motor, a power brake booster motor, a stability control pressure pump motor, or an HVAC pump motor. And in both cases, the sudden acceleration mode can disappear completely when the DC link voltage sensor is digitized again without a voltage spike being present, leaving no trace of hardware fault, software fault, or diagnostic trouble code (DTC). The accelerator pedal sensor reading in the EDR will not be changed by this faulty operation because it is likely taken from a signal that appears earlier in the controller chain of operations, such as before or after the pedal map. Therefore, if the accelerator pedal sensor reading in the EDR increases during a sudden acceleration incident, it will likely rule out sudden acceleration by this mechanism.

We will now consider a different controller design and analyze it to determine what happens when there is an error in the sensed value of $V_{\text{DCLink}}(\text{SOC})$ causing it to be much lower than the normal minimum value of $V_{\text{DCLink}}(\text{SOC})$.

Table 3. Summary of combined motor controller operations immediately after V_{DClk} changes to $V_{DClk}(\text{faulty})$ in the controller while the motor continues to operate with V_{DClk} unchanged. This causes the controller to conclude it must operate in the field weakening region while the motor remains operating in the base region. As a result, the controller applies the flux-adjusting operation associated with faulty V_{DClk} changes in the faulty field weakening region to the estimated flux of the motor in the base region, which does not change. The result is that the negative feedback to the PID controllers exceeds the set-point values by over 100 times, causing them to operate without negative feedback. This allows the outputs of the PID controllers to increase without bound, causing sudden unintended acceleration even if the driver has not stepped on the accelerator pedal.

	Base Region	Field Weakening Region
	If V_{DClk} changes to $V_{DClk}(\text{faulty})$ while the motor is operating in the base region, then operations using $V_{DClk}(\text{faulty})$ are performed on the combined motor/controller outputs in the base region with the motor still at the V_{DClk} value as shown in the previous table. The following two possibilities depend on the value of $V_{DClk}(\text{faulty})$.	
Combined Motor and Controller Operation	<ol style="list-style-type: none"> 1) Calculate $[V_{DClk}(\text{max})/V_{DClk}(\text{faulty})]$. 2) If $\omega \times [V_{DClk}(\text{max})/V_{DClk}(\text{faulty})] < \omega_{\text{base}}$, then the motor is operating in the faulty base region. 3) Set the λ^* set-point equal to the λ^{ref} output of the inverse motor map to keep the flux constant with ω and V_{DClk} in the faulty base region 4) Set the i_t^* set-point equal to T^{ref}/λ^* to keep the torque constant with ω and V_{DClk} in the faulty base region. 5) The i_t^{\wedge} and λ^{\wedge} feedback values from the motor should vary with V_{DClk} the same as the values i_t^* and λ^* 6) The base speed ω_{base} should decrease with $V_{DClk}(\text{faulty})$ 7) The motor flux and torque should not vary with ω or V_{DClk} in the faulty base region. [= > Motor runs normally in faulty base region] 	<ol style="list-style-type: none"> 1) Calculate $[V_{DClk}(\text{max})/V_{DClk}(\text{faulty})]$. 2) If $\omega \times [V_{DClk}(\text{max})/V_{DClk}(\text{faulty})] > \omega_{\text{base}}$, then the motor is operating in the faulty field weakening region 3) Apply field weakening to the the λ^{ref} output of the inverse motor map to obtain the λ^* set-point, making the flux vary with ω and $V_{DClk}(\text{faulty})$ in the faulty FW region. 4) Set the i_t^* set-point equal to T^{ref}/λ^* to make the torque vary with ω and $V_{DClk}(\text{faulty})$ in the faulty FW region. 6) The motor continues to run in the base region with the voltage $V_{DClk}(\text{SOC})$. Therefore, the feedback values i_t^{\wedge} and λ^{\wedge} from the motor will be independent of $V_{DClk}(\text{SOC})$ while the setpoints i_t^* and λ^* will vary with $V_{DClk}(\text{faulty})$, which are >100 times lower. Therefore, the PID controllers begin to operate without negative feedback, allowing the PID outputs to increase without bound. [= > Sudden Unintended Acceleration]

B. Motor and controller with the maximum torque in the base region limited by a PWM value that increases with decreasing DC link voltage.

As a motivation for understanding why one would use a PWM value that increases with decreasing DC link voltage, consider the waveforms shown in Figure 26 and the explanation given in the caption to Figure 26.

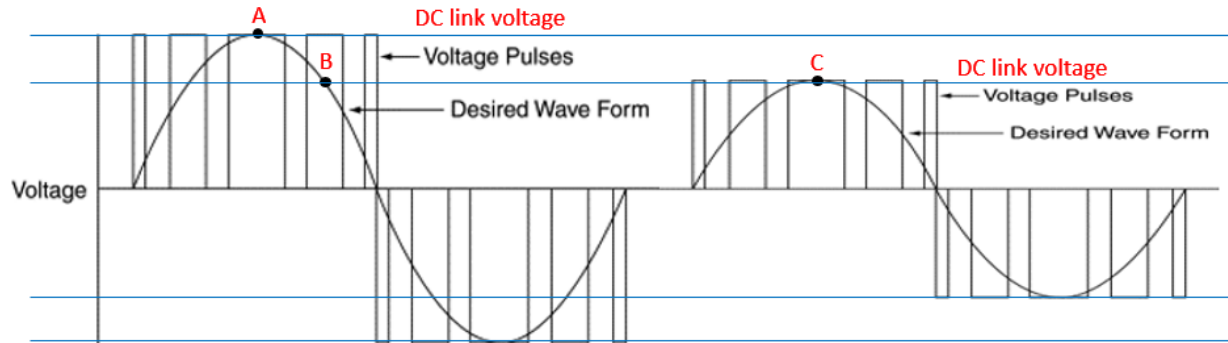


Figure 26. If the DC link voltage decreases with SOC without changing the PWM values (right waveform compared to left waveform), then the maximum voltage and all corresponding PWM voltages lower than the maximum voltage change by the same ratio. This shows if the maximum torque decreases as the DC link voltage decreases with SOC, then all torques derived from the maximum torque by PWM modulation also decrease with the DC link voltage as it decreases with SOC. Also, if one multiplies the PWM value of point B on in the left-hand waveform by the ratio of the DC link voltage of the left-hand waveform to the right-hand waveform, then point C in the right-hand waveform (which has the same voltage as B) changes back to point A in the left-hand waveform. This shows that by multiplying (i.e., boosting) the PWM values of all torques derived from a DC link voltage that changes with SOC by multiplying the PWM values by the inverse ratio that the DC link decreases with SOC, one can remove the SOC dependence of all the new PWM' values on the DC link voltage. This is how a maximum inverter torque can be obtained. And all lower torques obtained from it by using the boosted PWM' values also do not change with SOC value.

If one still needs convincing that this conclusion is correct, then consider Figure 27 and the explanation given in its caption.

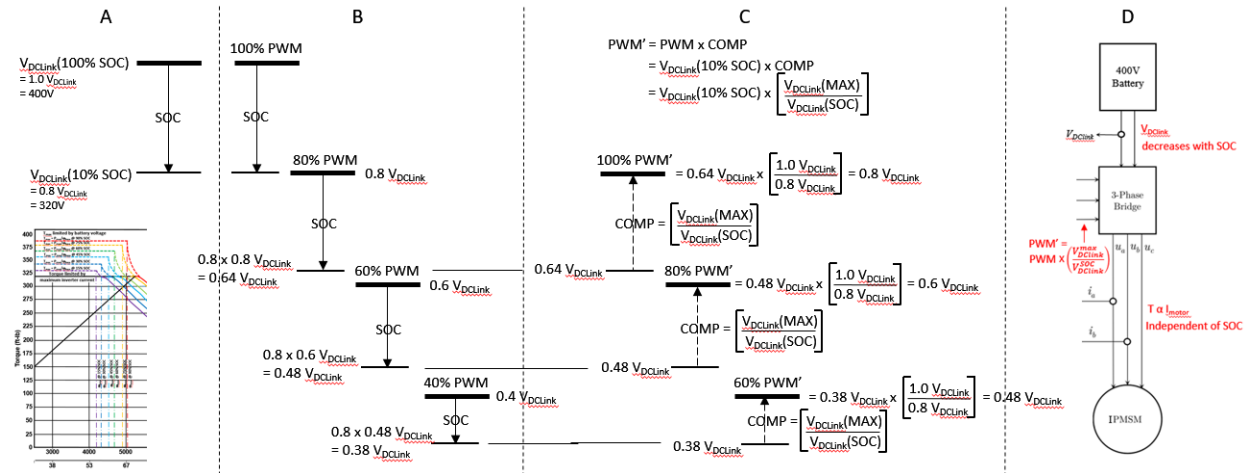


Figure 27. This figure shows how the maximum torque is limited by the inverter as shown in the inset figure in Column A when the inverter can only produce torques below some maximum by using PWM modulation to vary the current from the DC link to the motor. Usually, such currents below maximum will vary with the DC link voltage as it changes with SOC as shown in Column B. Column B clearly shows that if one just PWM's the DC link voltage, then all torques below 100% PWM will decrease by the same % as the DC link voltage decreases with SOC. So column B is not the solution. So is the maximum inverter current limited by some other technique outside the inverter? If so, then this other technique amounts to being a regulator of the DC link voltage and current. Some electric vehicles actually use such a DC link voltage regulator, but never battery-powered vehicles of the class being considered. Column C shows how the maximum inverter current is defined using PWM. Column C shows that if we select new PWM' values such that $PWM' = PWM \times COMP = PWM \times [V_{DCLink}(MAX) / V_{DCLink}(SOC)]$, then the new boosted PWM' values will increase with decreasing SOC causing the torques produced from a DC link voltage that decreases with SOC to be independent of SOC, as shown in Column D. This is one way that a battery-powered vehicle can limit the maximum inverter torque and how it can obtain torques lower than the maximum torque that do not change with the SOC of the battery voltage.

Let's now show what we have learned in the context of a block diagram of the vehicle's complete control system. Figure 28 shows on the right that if the DC link voltage produced by the high voltage battery decreases with SOC, then the motor torques produced from this DC link voltage by an inverter using PWM values that are independent of SOC produces voltages, currents, and torques that decrease as the SOC of the high voltage battery decreases.⁷ This variation of the motor torque with SOC value is not what we would like to see. The PWM values in this case are produced by the control electronics between the inverse motor map and the inverter based on set-points for the motor currents stored in the inverse motor map.⁸ These motor current set-points assume that the battery voltage is fixed at its maximum battery voltage of 400V. They are selected by torque requests that come from the pedal map, which also assumes that the torques are fixed relative to a battery voltage of 400V. This means they are independent of battery SOC. Finally, the torque requests are set by the driver pressing on the accelerator pedal, which varies the inputs to the pedal map that produce the requested torque outputs. Again, this control

⁷ Torques are produced by varying the motor currents. But the motor currents are proportional to the inverter output voltages, which are proportional to the input DC link voltage.

⁸ This is why the map is called an inverse motor map, because if a real motor maps input current values to output torques, then an "inverse motor" will map input torque requests to output motor currents.

[illegible]

Figure 29 shows a modified control system that achieves what is desired; namely, motor torques that do not decrease with a decrease in the DC link voltage as the SOC of the high voltage battery changes.

A Cause of Sudden Acceleration In Battery Powered Electric Vehicles – Rev 3

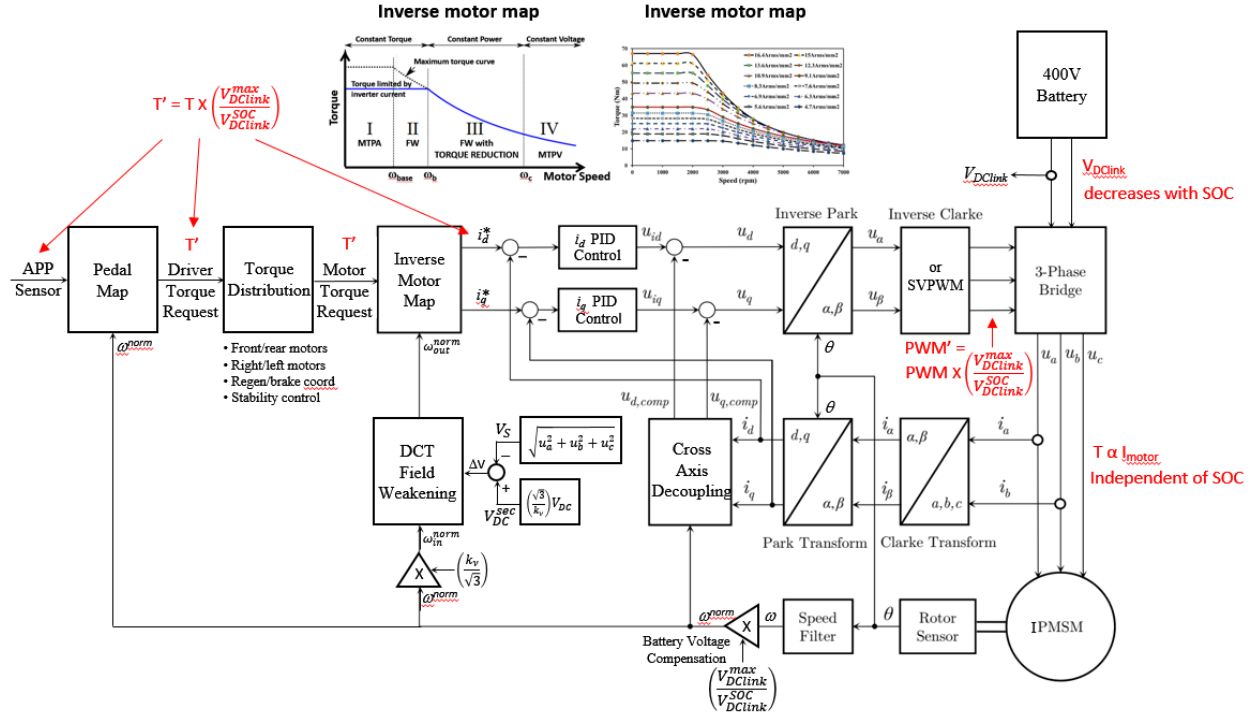


Figure 29. This figure shows a block diagram of the vehicle's complete control system which produces motor torques that are independent of the SOC of the high voltage battery. In this scheme the motor torques are produced by PWM' values that increase with SOC which exactly cancel the decreases in SOC associated with the DC link voltage that is being acted on. The

PWM' values that vary with SOC are obtained from the requested torques by boosting the requested torques by the ratio of $[V_{DClink}(MAX) / V_{DClink}(SOC)]$, where $V_{DClink}(SOC)$ is obtained by sensing the DC link voltage with a high voltage sensor. This boosting is done in one of three possible locations as shown in the figure. This control scheme yields motor torques that are independent of the SOC changes in the high voltage battery.

Therefore, in order to prevent the motor torque from decreasing as the DC link voltage decreases with the SOC of the high voltage battery, it is necessary to boost the requested torque by the inverse value $V_{DC}(MAX)/V_{DC}(\text{lower \% SOC})$ as shown in Figure 29. This can be done by multiplying the requested torque by $V_{DC}(MAX)/V_{DC}(\text{lower \% SOC})$ at one of three alternative places in the controller block diagram as shown in Figure 29: 1) after the inverse motor map, 2) after the pedal map, or 3) just before the pedal map. If done after the inverse motor map (alternative 1), this multiplication decreases the time available for other important operations on the requested torque. Therefore, it is usually done after the pedal map or just before the pedal map (alternatives 2 or 3). This boosting works well as long as the voltage $V_{DC}(\text{lower \% SOC})$ is measured correctly to correspond to the DC link voltage that the motor is actually seeing. But if the DC link voltage is measured incorrectly as a result of the mechanism discussed in Section II of this paper, then several adverse consequences will follow. We will now discuss these consequences.

Sudden Unintended Acceleration. The first adverse consequence of an incorrectly sensed DC link voltage $V_{DC}(\text{lower \% SOC})$ is unintended acceleration of the vehicle. This can happen without the driver's foot being on the accelerator pedal because the torque request to the drive motor is always being boosted by a small number to make the torque independent of the decrease in DC link voltage that accompanies a reduction in the SOC value of the high voltage battery. Usually this torque multiplier is between 1 and 1.33, which is the inverse of the ratio $V_{DC}(\text{lower \% SOC})/V_{DC}(\text{MAX})$ that the DC link voltage decreases due to a decrease in the SOC of the high voltage battery. But if the DC link voltage is sensed incorrectly due to a negative voltage spike occurring while the voltage is being digitized by an A/D converter as discussed in Section II, then the torque gets boosted by a number that can be up to a hundred times larger. This sudden change of the torque boost to a much larger number can cause the motor torque to suddenly increase from a low torque associated with parking lots and stop lights to a high torque associated with vehicle lurches over parking curbs and cruise speeds higher than the driver intends.

This sudden change in the boosted torque happens independently of whether or not the accelerator pedal is being depressed. It depends only on the voltage value obtained when the DC link voltage is digitized by the A/D converter, which occurs infrequently because the DC link voltage changes very slowly with the SOC of the high voltage battery. And since this torque boost multiplier $V_{DC}(\text{MAX})/V_{DC}(\text{lower \% SOC})$ is stored in digital memory and reused for boosting the torque until another voltage sample is taken later, the unintended acceleration can continue for several minutes unless it is ended earlier by the vehicle crashing into an object. No diagnostic trouble code (DTC) is ever found after an incident because no hardware or software fault is involved to cause this unintended acceleration. The only thing that changes to cause the unintended acceleration is a sensed DC link voltage value that decreases suddenly because it is digitized during a negative-going voltage spike. And no diagnostic is provided by any manufacturer that can detect this sudden change in the sensed DC link voltage because control system design engineers at most companies are unaware that these negative-going voltage spikes can occur. Since DC link voltage samples start being taken right after starting the vehicle, sudden voltage changes can occur more often at this time, causing more incidents to occur when the driver begins a trip or when the vehicle speed is low. For the same reason, an incorrectly sensed DC link voltage value stored in memory during an incident can be changed to a correctly sensed one when the vehicle is restarted, causing the unintended acceleration to be absent when the vehicle is restarted after an incident. Therefore, it is clear that the unintended acceleration is caused by the vehicle's control system and not by the driver pressing on the accelerator pedal.

The accelerator pedal % reading in the EDR can increase without the driver's foot being on the accelerator pedal. This can happen if the signal that is reported as the accelerator "pedal %" reading to the EDR is taken from a point in the signal flow after where the torque is boosted to make it independent of the SOC of the high voltage battery. This boosting must be done somewhere in all battery-powered electric vehicles or else the drive motor torque will decrease with a decrease in the SOC of the high voltage battery. This boosting of the torque can be done either after the pedal map or at the input to the pedal map as shown in Figure 29. In the latter case, it is done after all other tests and checks have been performed on the two APP sensor signals, and after a single % full depression value has been obtained that is used as an input to the pedal map.

Either signal location is acceptable for use as the accelerator "pedal %" reading in the EDR because both the current EDR regulation and the proposed new EDR regulation allow reporting either the engine "throttle %" signal or the accelerator "pedal %" signal to be used as the accelerator "pedal %" signal (see Figures 31 and 32). In an electric vehicle, the requested torque signal provided by the pedal map serves the same function as the engine "throttle %" signal in an ICE vehicle. Therefore, three combinations of torque boosting and pedal sensor reading are

possible: 1) torque boosting followed by “pedal %” signal reading are both done on the single input signal to the pedal map, 2) torque boosting followed by “pedal %” signal reading are both done on the single output signal from the pedal map, and 3) torque boosting is done on the single input signal to the pedal map followed by “pedal %” signal reading done on the single output signal from the pedal map.

Any one of these three combinations will provide an EDR accelerator “pedal %” reading that increases without the driver pressing on the accelerator pedal when the motor torque is boosted by an incorrectly sensed DC link voltage that causes unintended acceleration. This fact belies the belief that sudden acceleration in an electric vehicle is caused only by the driver pressing on the accelerator pedal if the EDR “pedal %” reading is non-zero, and offers a specific mechanism for getting non-zero accelerator “pedal %” EDR data despite all the redundancy and checks performed on the outputs of the dual accelerator pedal sensors. The answer is simply that during unintended acceleration the normal torque boost that is used to obtain a motor torque that is independent of the battery SOC is increased to an abnormally high value by an incorrectly sensed DC link voltage value, followed by the EDR taking the “pedal %” signal from the torque signal at a point downstream from where the torque is boosted.

Table II-1
Required Essential Data Elements and Formats

Item #	Data Elements	Recording Time*	Sampling Rate	Range	Accuracy	Resolution	Filter
1	Delta-V, Longitudinal	0 – 250 ms	100/s	-100 to 100 km/h	± 5%	1 km/h	N.A.
2	Maximum delta-V, Longitudinal	0 – 300 ms	N.A.	-100 to 100 km/h	± 5%	1 km/h	N.A.
3	Time, Maximum delta-V, Longitudinal	0 – 300 ms	N.A.	0 – 300 ms	± 3 ms	2.5 ms	N.A.
4	Speed, vehicle indicated	-5.0 to 0 s	2/s	-200 to 200 km/h	± 1 km/h	1 km/h	N.A.
5	Engine throttle, % full (accelerator pedal % full)	-5.0 to 0 s	2/s	0 – 100%	± 5%	1%	N.A.
6	Service brake, on/off	-5.0 to 0 s	2/s	On/off	N/A	N/A	N/A
7	Ignition cycle, crash	-1.0 s	N.A.	0 – 60,000	± 1 cycle	1 cycle	N.A.
8	Ignition cycle, download	At time of download	N.A.	0 – 60,000	± 1 cycle	1 cycle	N.A.
9	Safety belt status, driver	-1.0 s	N.A.	On/off	N/A	On/off	N.A.
10	Frontal air bag warning lamp	-1.0 s	N.A.	On/off	N/A	On/off	N.A.
11	Frontal air bag deployment time, Driver (1 st stage, in case of multi-stage air bags)	Event	N.A.	0 – 250 ms	± 2 ms	1 ms	N.A.
12	Frontal air bag deployment time, RFP (1 st stage, in case of multi-stage air bags)	Event	N.A.	0 – 250 ms	± 2 ms	1 ms	N.A.
13	Multi-event, number of events (1 or 2)	Event	N.A.	1, 2	N/A	1, 2	N.A.
14	Time from event 1 to 2	As needed	N.A.	0 – 5.0 s	0.1 s	0.1 s	N.A.
15	Complete file recorded (yes or no)	After Other Data	N.A.	Yes/no	N/A	Yes/no	N.A.

s: second; ms: millisecond; km/h: kilometer per hour; RFP: right front passenger; N.A.: not applicable
* Relative to time zero

Figure 31. NHTSA’s current EDR regulations allow either the engine throttle reading or the accelerator pedal reading to be used as the EDR accelerator pedal sensor reading.^[13]

Sudden acceleration can occur during autopilot mode as well as non- autopilot mode operation. Sudden acceleration can occur during autopilot mode operation because the requested torque commands in this mode, which are generated by the autopilot’s torque controller, must be corrected for the reduction in torque caused by a decrease in the DC link voltage with a decrease in SOC of the high voltage battery, just as the driver-requested torque commands in the non-autopilot mode must be corrected. This boosting operation works well as long as the voltage V_{DC} (lower % SOC) is measured correctly to correspond to the voltage that the motor is actually seeing. But if this boosting is changed by incorrectly sensing the DC link voltage value as a result of the mechanism discussed in Section II of this paper, then the adverse consequences of: a) unintended acceleration with the driver’s foot off the accelerator pedal, and b) the accelerator “pedal %” reading in the EDR increasing without the driver’s foot being on the accelerator pedal, will follow.

TABLE I—DATA ELEMENTS REQUIRED FOR ALL VEHICLES EQUIPPED WITH AN EDR

Data element	Recording interval/time ¹ (relative to time zero)	Data sample rate (samples per second)
Delta-V, longitudinal	0 to 250 ms or 0 to End of Event Time plus 30 ms, whichever is shorter	100
Maximum delta-V, longitudinal	0-300 ms or 0 to End of Event Time plus 30 ms, whichever is shorter	N/A
Time, maximum delta-V	0-300 ms or 0 to End of Event Time plus 30 ms, whichever is shorter	N/A
Speed, vehicle indicated	-20.0 to 0 sec	10
Engine throttle, % full (or accelerator pedal, % full)	-20.0 to 0 sec	10
Service brake, on/off	-20.0 to 0 sec	10
Ignition cycle, crash	-1.0 sec	N/A
Ignition cycle, download	At time of download ²	N/A
Safety belt status, driver	-1.0 sec	N/A
Frontal air bag warning lamp, on/off ³	-1.0 sec	N/A
Frontal air bag deployment, time to deploy, in the case of a single stage air bag, or time to first stage deployment, in the case of a multi-stage air bag, driver	Event	N/A
Frontal air bag deployment, time to deploy, in the case of a single stage air bag, right front passenger	Event	N/A
Multi-event, number of event	As needed	N/A
Time from event 1 to 2	Following other data	N/A
Complete file recorded (yes, no)		

¹Pre-crash data and crash data are asynchronous. The sample time accuracy requirement for pre-crash time is -0.1 to 1.0 sec (e.g., T = -1 would need to occur between -1.1 and 0 seconds).
²The frontal air bag warning lamp is the readiness indicator specified in S4.5.2 of FMVSS No. 208, and may also illuminate to indicate a malfunction in another part of the deployable restraint system.
³The ignition cycle at the time of download is not required to be recorded at the time of the crash, but shall be reported during the download process.

Figure 32. NHTSA’s proposed EDR regulations for 2023 allow either the engine throttle reading or the accelerator pedal reading to be used as the EDR accelerator pedal sensor reading.^[14]

We conclude this analysis with a review of what has been found. It has been found that with this scheme the requested torque is always boosted (i.e., multiplied) by the same ratio that the DC link voltage decreases with SOC. This explains:

- 1) How the maximum torque below base speed is made independent of SOC by sensing the DC link voltage and then boosting the PWM values by the same ratio as the DC link voltage decreases due to SOC.
- 2) How this boosting is done to the requested torque after the pedal map or just before the pedal map, where there is only one signal line with no redundancy.
- 3) How sudden unintended acceleration happens without the driver stepping on the accelerator pedal when the boosting is done using an incorrect DC link voltage that is digitized during a negative-going voltage spike caused by the inrush current of an electric motor turning on, such as the electric power steering motor, the electric brake booster motor, or the HVAC motor.
- 4) How the EDR accelerator “pedal %” reading is increased without the driver’s foot being on the accelerator pedal, because it is taken from a point in the signal flow after where the torque is boosted to make it independent of the SOC of the high voltage battery.
- 5) How sudden acceleration can occur during autopilot mode operation as well as non-autopilot mode because the requested torque commands in autopilot mode, which are generated by the autopilot’s torque controller, must be corrected for the reduction with SOC just as the driver-requested torque commands in the non-autopilot mode must be corrected.

The findings in this case belie the belief that sudden acceleration in an electric vehicle is caused only by the driver pressing on the accelerator pedal if the EDR “pedal %” reading is non-zero. They offer a specific mechanism for sudden unintended acceleration without the driver stepping on the accelerator pedal and for getting a non-zero accelerator “pedal %” EDR data despite all the redundancy and checks he describes on the outputs of the dual accelerator pedal sensors. The answer not that the redundancy and checks on the accelerator pedal signals are wrong frequently assumed. The answer is simply that all these checks and redundancy are irrelevant to the cause of sudden unintended acceleration in this case because sudden unintended acceleration is not caused by the driver stepping on the accelerator pedal. Instead, it is caused by the normal torque boost that is used to obtain a motor torque that is independent of the battery SOC being increased to an abnormally high value by an incorrectly digitized DC link voltage value, followed by the EDR taking the “pedal %” signal from the torque signal at a point downstream from where the torque is boosted.

These findings provide sufficient evidence for sudden unintended acceleration in battery-powered electric vehicles of the class defined in Section I that NHTSA and the courts should allow plaintiffs during discovery to review the manufacturer’s motor controller source code to determine whether boosting of the requested torque is being done to remove the dependence of torque on the SOC of the high voltage battery and to determine whether the EDR accelerator “pedal %” reading is taken from a point in the signal flow after where the torque is boosted. If these design features are found, as predicted by the findings of this paper, then the manufacturers should be found responsible for the sudden unintended acceleration events claimed by the plaintiffs, as well as by previous plaintiffs who had their claims denied because the manufacturer insisted that sudden unintended acceleration was impossible in their vehicles unless the driver pressed on the accelerator pedal.

C. Summary of Section III Results.

In this section two different controller designs were analyzed to determine how they behaved when an error occurred in the DC link voltage. In both cases sudden unintended acceleration occurred in both the driver-controlled mode and the autopilot mode without the driver’s foot

being on the accelerator pedal. In both cases and both designs, sudden acceleration can occur randomly when a negative-going voltage spike happens to occur at the time the DC link voltage sensor is digitized, which may coincide with some motor turning on, such as a power steering boost motor, a power brake booster motor, a stability control pressure pump motor, or an HVAC pump motor. And in both cases and both designs, the sudden acceleration mode can disappear completely when the DC link voltage sensor is digitized again without a voltage spike being present, leaving no trace of hardware fault, software fault, or diagnostic trouble code (DTC). However, the accelerator pedal sensor reading in the EDR behaves differently in the two designs. In the first design it will not be changed during faulty controller operation unless the driver presses on the accelerator pedal because it is likely derived from a signal that appears earlier in the controller chain of operations, such as before or after the pedal map. In the second design it is possible for it to increase without the driver's foot being on the accelerator pedal during faulty controller operation because it is likely derived from a signal after the signal has been changed by the faulty controller operation. One can determine which controller design applies in a given vehicle incident by performing a dynamometer test to check how the torque behaves with changes in the SOC of the high voltage battery. If the torque changes with battery SOC, then the first controller design applies. If it does not change with battery SOC, then the second controller design applies. These results show that it is important to analyze any new controller design in a similar fashion to determine how it behaves during faulty controller operation.

IV. Elimination of Sudden Acceleration

Knowing that sudden acceleration is caused by negative voltage spikes on the 12V battery bus that change the output of the DC link sensor allows one to come up with possible mitigation measures for eliminating the sudden acceleration. Adding more capacitance to the 12V supply line to eliminate the large negative-going voltage spikes is futile because the inrush currents are so high. But the following techniques for dealing with the spikes may be considered:

- 1) Test the sampled voltage of the high voltage battery before using it and then do one of the following:
 - a. If the sampled battery voltage is found to be less than some normal voltage like 300V, then don't change the supply voltage from the previous value.
 - b. If the sampled battery voltage is found to be less than some normal voltage like 300V, then use some default battery voltage like 300V instead.
 - c. If the sampled battery voltage is found to be less than some normal voltage like 300V, then resample the battery voltage and again compare it to some normal battery voltage like 300V. Then use it only if it exceeds 300V.
- 2) Take two samples of the voltage of the high voltage battery about 1 millisecond apart. Then compare the two samples and use the higher voltage sample.
- 3) Add a circuit to the input of the power steering motor that limits the inrush current to the motor during start-up until after the magnetic field in the motor has built up.

Only by eliminating the negative-going spikes on the 12V supply bus, or by preventing them from affecting the sampling of the DC link voltage sensor output, will one be successful in eliminating the sudden acceleration caused by this mechanism.

V. Summary of the Proposed Cause of Sudden Acceleration in BeV's

A cause of sudden unintended acceleration in a generic class of battery-powered electric vehicles (BeV's) having similar design features has been discussed. The cause is associated with the voltage compensation algorithm used in all such vehicles to correct the motor operating point for changes in DC link voltage that accompany changes in the state of charge (SOC) of the high voltage battery. Normally this battery voltage compensation causes an increase in the motor speed of 25% or less that corrects for the decrease in motor speed caused by a lower battery

voltage due to a decrease in the SOC. But when the battery voltage is sensed during a negative voltage spike caused by the inrush current of an electric motor turning on, then an incorrect DC link voltage reading results that causes the standard compensation algorithm to increase the motor speed by over 300x. This condition persists until another DC link voltage reading is taken many minutes later. In the meantime, the motor operating point associated with a released accelerator pedal is suddenly increased to an operating point in the field weakening region. If the existing motor stator voltage then exceeds the incorrectly sensed DC link voltage, then an unstable condition exists in the control electronics in which control of the motor operating point is lost. The motor torque can then increase without control, resulting in sudden unintended acceleration without the driver pressing on the accelerator pedal. Measures have been proposed to eliminate the sudden acceleration by testing the DC link voltage immediately after sampling and limiting it to less than the maximum 25% change normally seen from the maximum battery voltage of 400V.

In this revision two different controller designs were analyzed to determine how they behaved when an error occurred in the DC link voltage. In both cases sudden unintended acceleration can occur in both the driver-controlled mode and the autopilot mode without the driver's foot being on the accelerator pedal. In both cases and both designs, sudden acceleration can occur randomly when a negative-going voltage spike occurs at the time the DC link voltage sensor is digitized, which may coincide with some motor turning on, such as a power steering boost motor, a power brake booster motor, a stability control pressure pump motor, or an HVAC pump motor. And in both cases and both designs, the sudden acceleration mode can disappear completely when the DC link voltage sensor is digitized again without a voltage spike being present, leaving no trace of hardware fault, software fault, or diagnostic trouble code (DTC). However, the accelerator pedal sensor reading in the EDR behaves differently in the two designs. In the first design it will not be changed during faulty controller operation unless the driver presses on the accelerator pedal because it is likely derived from a signal that appears earlier in the controller chain of operations, such as before or after the pedal map. In the second design it is possible for it to increase without the driver's foot being on the accelerator pedal during faulty controller operation because it is likely derived from a signal after the signal has been changed by the faulty controller operation. One can determine which controller design applies in a given situation by performing a dynamometer test to check how the torque behaves with changes in the SOC of the high voltage battery. If the torque changes with battery SOC, then the first controller design applies. If it does not change with battery SOC, then the second controller design applies. These results show that it is important to analyze any different controller design in a similar fashion to determine how it behaves during faulty controller operation.

Appendix A. An Alternate Control System Diagram

Figure A.1 shows an alternate control system block diagram using (i_d^*, i_q^*) reference coordinates instead of (torque, flux) reference coordinates. This control system design avoids the need to estimate the stator flux in the feedback path from the stator voltages and currents to the input of the flux PID controller as seen in Figure 1 of this paper. It also includes a cross-axis decoupling capability that removes effects in either the i_d or i_q channel caused by terms in the other channel. Otherwise, this design includes all the functions found in Figure 1 including field weakening, MTPV voltage reduction, and battery voltage compensation, and all the discussion associated with Figure 1 applies to this design also. This design is a usable alternative to the design of Figure 1 in any vehicle in the class of BeV's discussed. It was placed in this Appendix only to allow a more coherent discussion of the block diagram shown in Figure 1 of the paper.

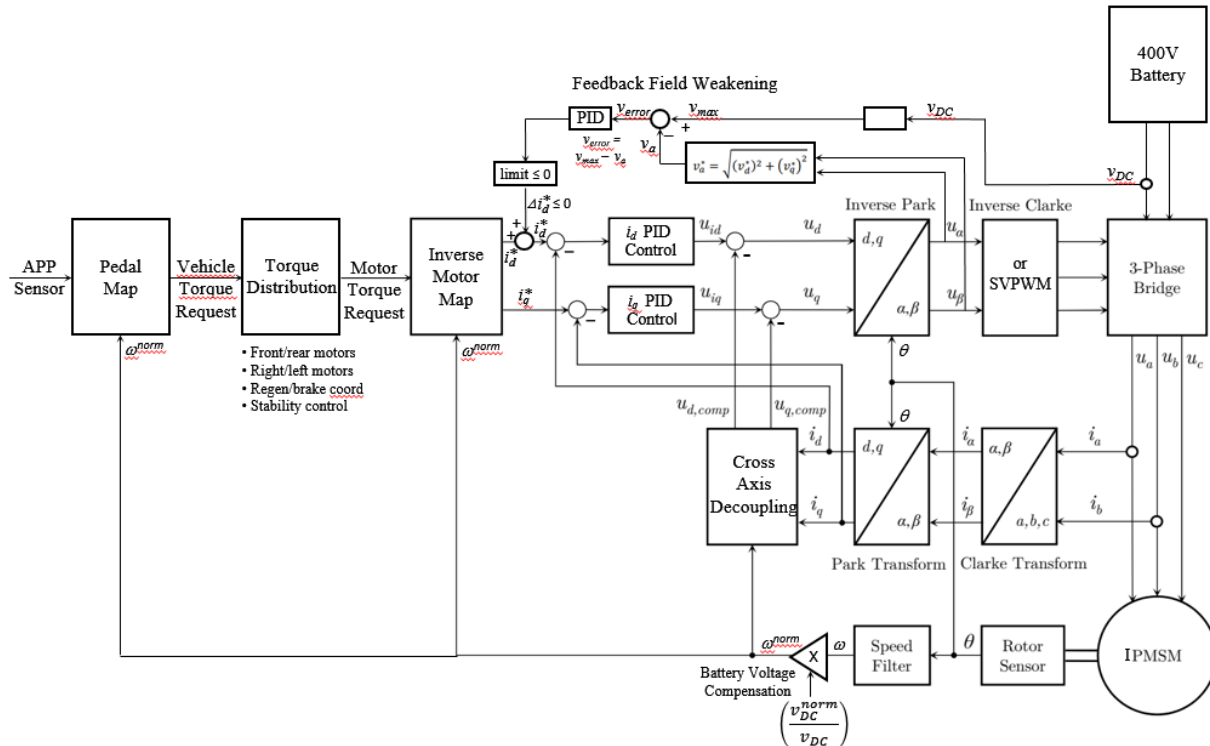


Figure A.1. Alternate control system diagram using (i_d^*, i_q^*) reference coordinates

Appendix B. Torque Curve Displacements Caused by Battery Voltages Sampled During a Voltage Spike

Figure 6, repeated below, explained how the torque curves shift to lower motor speeds as the battery voltage is lowered due to decreases in the battery state of charge (SOC). If the torque at lower motor speeds is limited by the maximum inverter current, then all the torque curves will have the same maximum torque. But if the torque at lower motor speeds is limited by the battery voltage, then the torque curves will shift downward as the battery voltage decreases with SOC. Therefore, by adjusting the maximum inverter current to limit the torque to values below the torque associated with a minimum value of 0% SOC, decreases in the maximum torque values of the curves with lower battery voltage can be masked. Under normal conditions of vehicle operation this setting of a maximum inverter current works to mask the variations of torque with battery voltage because the battery voltage cannot decrease any further after SOC has reached a zero percent state of charge.

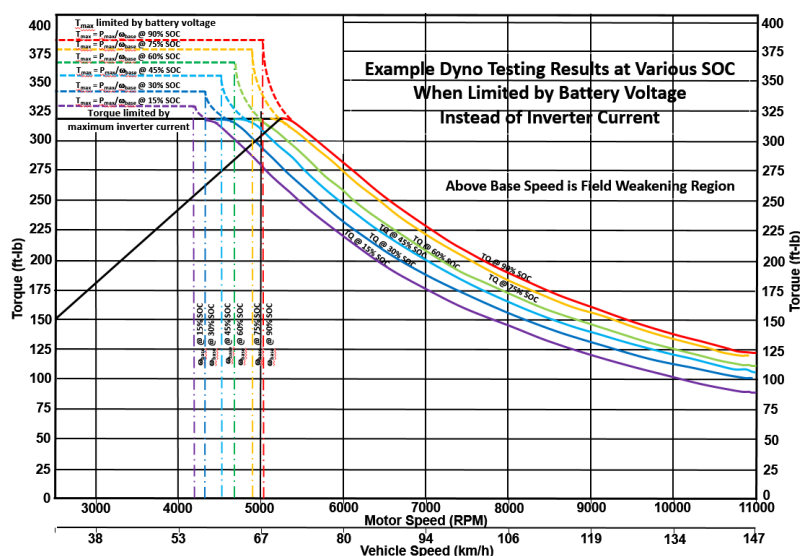


Figure 6. If the torque curves in Figure 5 were limited by battery voltage instead of inverter current, then the same data would look like this, showing that the speed shifts in the torque curves are caused by battery voltage changing as a result of SOC changes.

But if a negative voltage spike can cause the A/D converter to incorrectly sense a battery voltage that is lower than the normal value at 0% SOC, then the lower battery voltage detected by the A/D will cause the control system to believe that the torque curve has shifted to a much lower voltage. In this case, the maximum inverter current no longer masks the changes in torque with decreasing (incorrect) battery voltage. So the torque curves will shift again to lower torque values with decreasing (incorrect) battery voltage as shown in Figure B.1. This implies that the maximum torque becomes limited to a very low torque value when the battery voltage is sensed during a negative voltage spike. This produces no change, however, in how the control system reacts to the motor operating point. It still translates the motor operating point to a higher motor speed based using the ratio of the normal battery voltage (400V) to the incorrectly sampled battery voltage (near 0V). This causes an increase in motor speed of nearly 400x, which places the new operating point in the field weakening region with torque reduction. The field weakening algorithm then compares the stator voltage to the (incorrectly digitized) battery voltage. And if the stator voltage exceeds the (incorrectly digitized) battery voltage, then the

control system concludes that the motor operating point is in an unstable region where the motor torque can increase without limit.

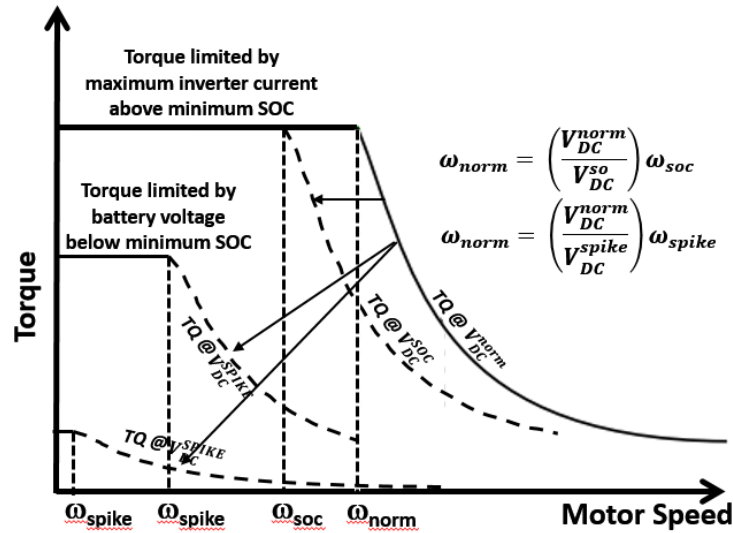


Figure B.1. When the battery voltage continues to decrease below the minimum SOC limit as a result if the A/D (incorrectly) digitizing the battery voltage during a negative voltage spike, then torque curves are no longer limited by the maximum inverter current. Therefore, their decrease in torque with decreasing battery voltage becomes visible, and one can see that that the maximum torque becomes limited to a very low torque value when the battery voltage is sensed during a negative voltage spike. This situation may not be anticipated by some control system designers.

Appendix C. Dynamic Effects Contributing to the Loss of Motor Control in the Field Weakening Region

When the voltage of the high voltage battery is sensed while the power supply of the high voltage sensor is being lowered by a negative voltage spike, it causes a sudden large decrease in the sensed battery voltage that creates a sudden large increase in the compensated motor speed. This causes the motor map to suddenly shift the operating point of the motor from an operating point near the origin of the base region to an operating point just inside the field weakening region. In this case, if the applicable field weakening voltage controller can't adjust the stator voltage fast enough to keep it below the suddenly lowered sensed battery voltage, then the current regulator in the main FOC control loop will saturate to cause a loss of motor control. This does not happen if the change in battery voltage is small, which keeps the operating point out of the field weakening region, as happens during a decrease in the battery voltage due to a change in the battery state of charge (SOC). It also does not happen if the change in battery voltage is large but slow, because the voltage controller in the field weakening control loop can then keep up with the slowly changing battery voltage. This implies that the loss of motor control happens because of a dynamic effect in which the voltage controller in the field weakening control loop can't keep up with a rapid change in the sensed battery voltage.

That a loss of motor control can be caused by a dynamic effect in the field weakening voltage control loop is explained more clearly in a paper entitled "*Design Criteria for Flux-Weakening Control Bandwidth and Voltage Margin in IPMSM Drives Considering Transient Conditions*" by Jose Jacob, Sandro Calligaro, Omar Botessi and Roberto Petrella.^[15] In this paper, the authors explain that field weakening in IPMSM motors is nearly always done using a feedback algorithm because feed-forward algorithms can fail due to their sensitivity to constantly changing motor parameters. They then do a stability analysis of the feedback control loop in the field weakening algorithms and find that, regardless of the exact feedback parameters used, all feedback algorithms require multiple passes through the feedback control loop to reach their intended voltage value. This takes a certain amount of time to converge. If this convergence time is greater than the time it takes for the sensed battery voltage to change, then the field weakening algorithm can't keep up with the change in the battery voltage and the current controller in the main FOC control loop saturates, causing a loss of motor control. The authors discuss three cases in which this effect causes a loss of motor control: 1) when the DC link voltage of the inverter is reduced suddenly while the motor is already in the field weakening region, 2) when the motor enters the field weakening region while undergoing a constant acceleration in motor speed, and 3) when the motor torque is suddenly changed while operating in the field weakening region. They then show how the algorithms perform in each case by both computer simulation and experimental results on an example IPMSM motor. Their simulation results agree with the experimental results in all three cases.

Figure 1 shows what happens when the DC link voltage is reduced while the motor is in the field weakening region. The top plot shows the DC link voltage (i.e., the sensed battery voltage) as a dashed black line and the motor's reference stator voltage (i.e., the intended stator voltage or nominal stator voltage) as a solid blue line. The two voltages differ by a voltage margin chosen by the designer to prevent the motor from operating in the "forbidden" area above the DC link voltage where the stator voltage becomes saturated. In between these two voltages is the actually measured stator voltage shown by a solid red line. This actual stator voltage differs from the reference stator voltage because it takes time for it to converge to the reference stator voltage. Therefore, there is a delay in the actual stator voltage relative to the reference stator

voltage. This delay causes the actual stator voltage to exceed the reference stator voltage by some control error, which reduces the voltage margin. The bottom plot shows how the voltage margin changes as the battery voltage changes. In this case the control error of about 10 volts reduces the voltage margin from the desired value of 25 volts to about 15 volts, changing back to 25 volts when the battery voltage stops changing.

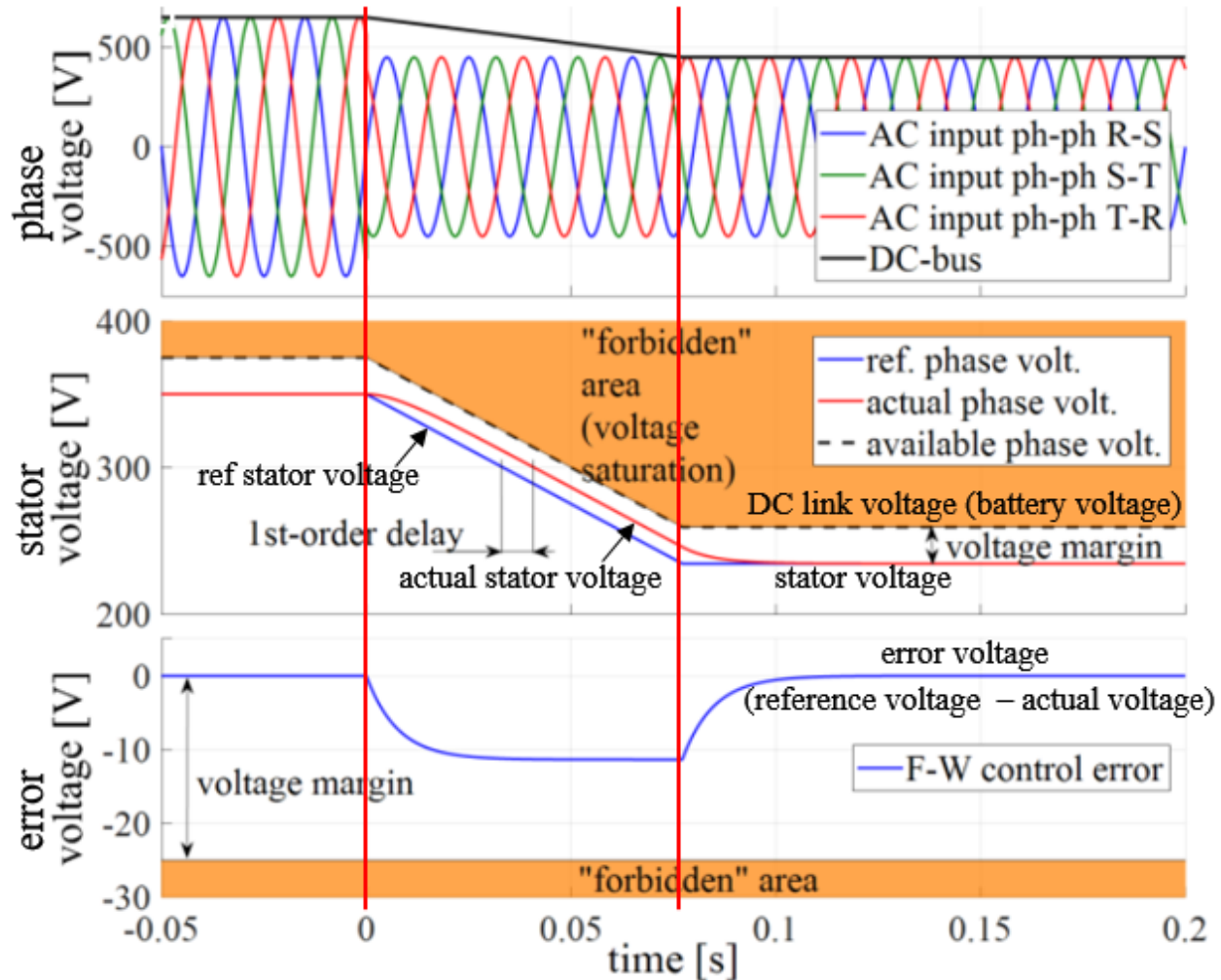


Figure 1. When the DC link voltage changes while the motor is in the field weakening region there is a delay in the stator voltage changing that produces a reduction of the voltage margin. This can cause a loss of motor control if the stator voltage becomes equal to the DC link voltage causing the voltage margin to go to zero.

Figure 2 shows experimental results on an IPMSM motor as the DC link voltage changes while the motor is in the field weakening region. In Figure 2a, when the battery voltage change takes place over a 0.07 sec time interval, the control voltage error reaches about 20V, which still leaves a 10V voltage margin. In Figure 2b, when the same decrease in battery voltage takes place over a shorter 0.04 sec time interval, the control voltage error reaches a larger value of about 30V, which leaves no voltage margin remaining. In this case, control of the motor is lost.

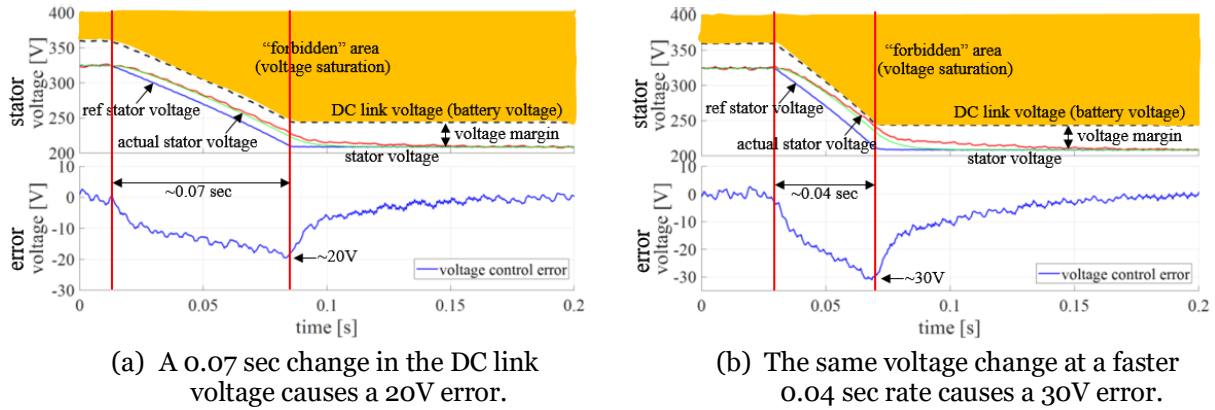


Figure 2. When the DC link voltage changes while the motor is in the field weakening region the error voltage increases as the voltage change occurs faster with the same size voltage change.

Figure 3 shows experimental results on an IPMSM motor when the motor enters the field weakening region while undergoing a constant acceleration in motor speed. The top plot shows the change in motor speed with time. The bottom plot shows when the speed enters the field weakening region at $t=0$ and the subsequent changes in the reference and actual stator voltages with time. The dashed black line shows the DC link voltage, the solid blue line shows the reference stator voltage, the solid red lines show the actually measured stator voltage for two cases of feedback loop timing. The red lines show that an actual stator voltage initially overshoots the reference stator voltage, and then converges slowly back to the reference stator voltage. The red line labelled 30 HZ BW has an overshoot of about 12V, leaving it with a 16V voltage margin, while the red line labelled 15 Hz BW has an overshoot of about 25V, leaving it with a 2V voltage margin. The solid green lines show the theoretical stator voltage assuming a simple one pole for the field weakening voltage control loop. The experimentally observed red lines follow the theoretical green lines closely and confirm that a higher bandwidth for the control loop results in a faster convergence time for the actual stator voltage to approach the reference stator voltage, resulting in a higher voltage margin for the stator voltage to remain under the DC link voltage.

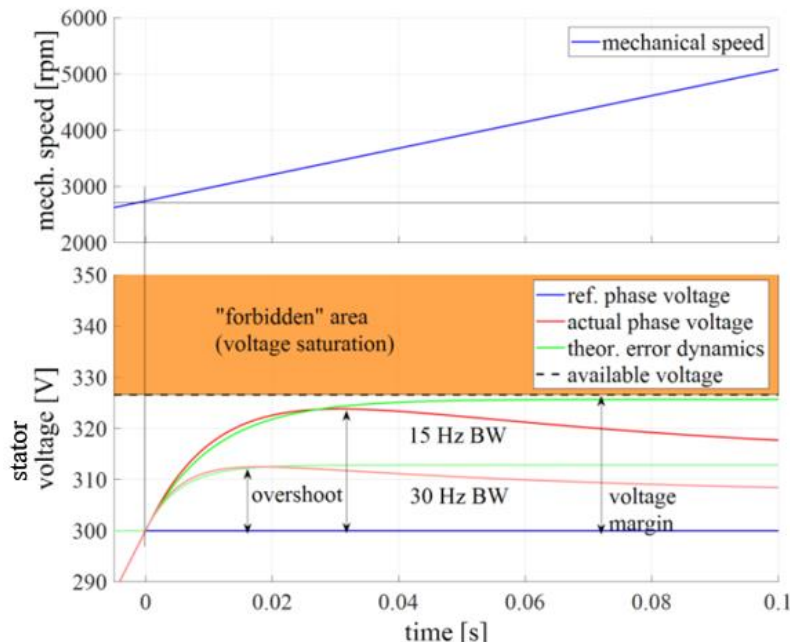


Figure 3. When the motor enters the field weakening region while undergoing a constant acceleration in motor speed, the actual stator voltage can overshoot the desired reference voltage causing a lowering of the voltage margin. This can cause a loss of motor control if the stator voltage becomes equal to the DC link voltage causing the voltage margin to go to zero.

Figure 4 shows experimental results on an IPMSM motor when the motor torque is suddenly changed while operating in the field weakening region. The top plot shows that the motor speed remains constant with time. The middle plot shows two cases of changing torque; the solid grey line is the case where the torque changes instantaneously, and the solid blue line where the change in torque is slowed down by a low pass filter. The bottom plot shows how the stator voltage changes when the torque is changed by the two changes in torque shown above. The dashed black line shows the DC link voltage and the solid blue line shows the desired reference stator voltage. They differ by a voltage margin chosen by the designer to ensure that the stator voltage does not exceed the DC link voltage. The dotted orange line is the experimentally measured stator voltage corresponding to an instantaneous change in torque. One sees that it exceeds the desired reference stator voltage by a large amount, leaving no voltage margin remaining. This allows the current regulator in the FOC control loop to saturate, causing a loss of motor control. The solid red line in the plot is the measured stator voltage that corresponds to the solid blue torque line above when the torque is slowed down by a low pass filter. One sees that the filter in the torque command slows down the disturbance and allows the slower-changing stator voltage signal to react and follow the faster torque signal more closely. With a torque filter, the stator voltage remains below the DC link voltage by a margin that is less than the desired voltage margin, but that still leaves some voltage margin remaining. The solid green line shows the theoretical stator voltage for this case, and it is very close to the actually measured stator voltage.

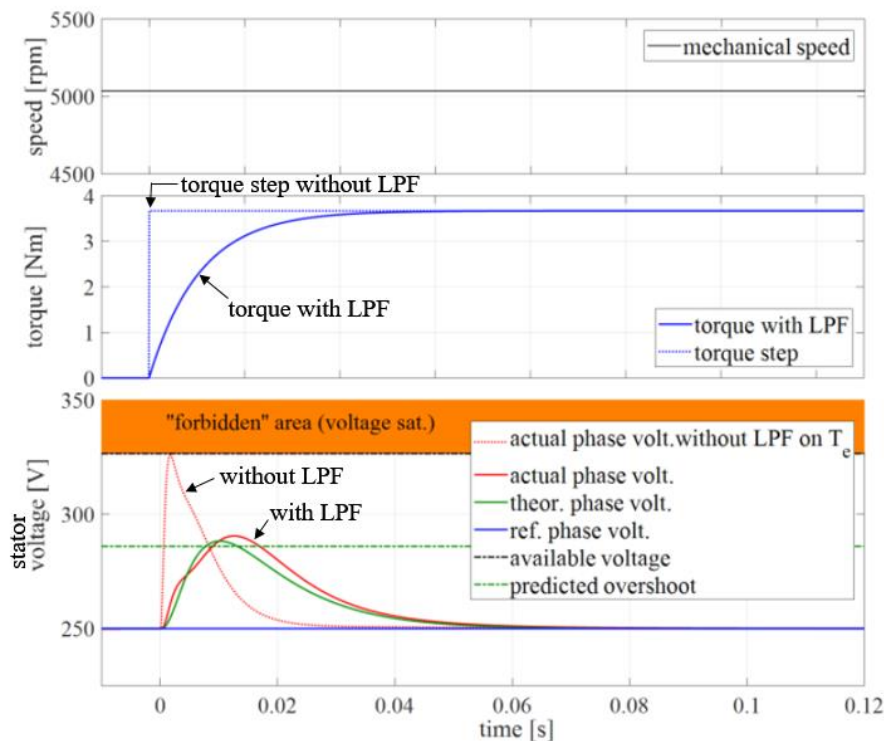


Figure 4. When the motor torque is suddenly changed while operating in the field weakening region, the actual stator voltage can overshoot the desired reference voltage causing a lowering

of the voltage margin. This can cause a loss of motor control if the stator voltage becomes equal to the DC link voltage causing the voltage margin to go to zero.

Figure 5 shows a conceptual plot for the case where the motor speed changes instantaneously from a point near zero speed to a point in the field weakening region. This is what happens when the voltage of the high voltage battery is sensed during a negative voltage spike, causing a sudden large decrease in the sensed battery voltage that creates a sudden large increase in the compensated motor speed. The overshoot in the stator voltage in this case is even greater than that shown in Figure 3 because of the suddenness of the motor speed change. In this case the larger overshoot causes the voltage margin to decrease even faster than shown in Figure 3. This is believed to be what happens during sudden unintended acceleration.

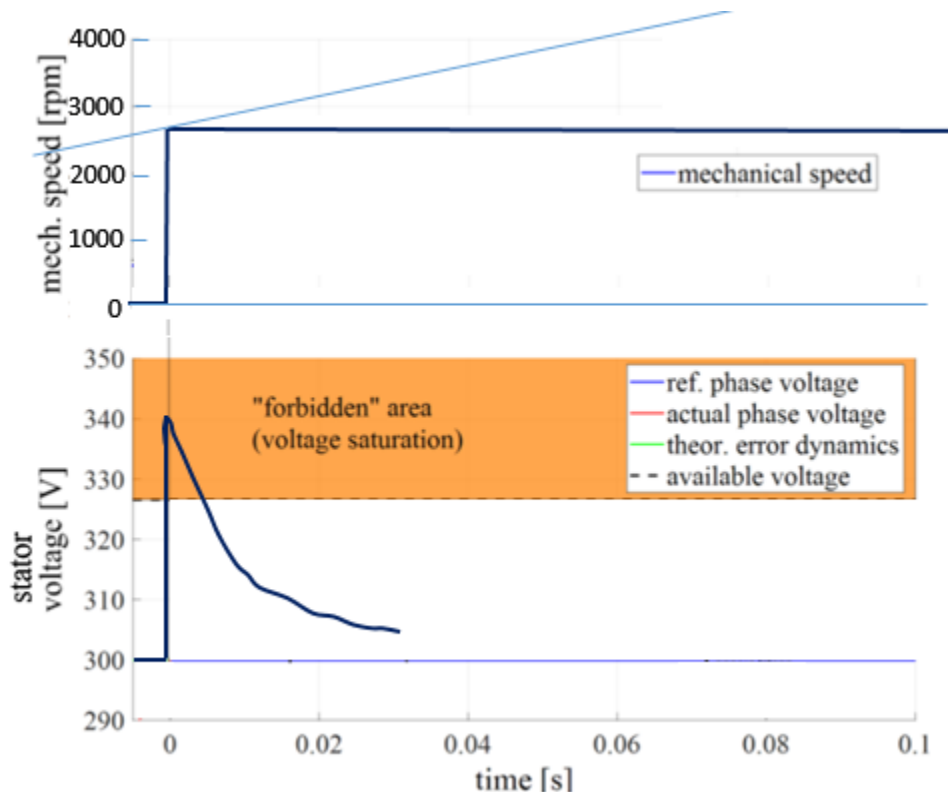


Figure 5. When the motor speed changes instantaneously from near zero to a point in the field weakening region, the overshoot in the stator voltage is even greater than that shown in Figure 3, causing the voltage margin to decrease to zero faster than shown conceptually in Figure 3. This is believed to be what happens during sudden unintended acceleration.

Appendix D. Feed-Forward Field Weakening Algorithms are Also Susceptible to Instability Causing Sudden Unintended Acceleration

Appendix C assumes that field weakening is done using a feedback algorithm in which the motor stator voltage approaches its new operating value slowly as the parameter values are changed. However, auto manufacturers may prefer to do field weakening by a feed-forward algorithm because it allows the drive motor to react faster to changes in the operating conditions, like driver commands and environmental conditions. This is often referred to as providing a better dynamical response to the drive motor, which allows it to respond faster to driver torque commands.

While giving a better dynamical response, a feed-forward algorithm also can also encounter the problem of unstable operation even when care is taken to use algorithms based on the most complex models that include all the possible motor parameters that can change. This is because motor parameters can sometimes go out of their expected range of operation, which may cause the PID controller for the stator current to saturate, causing a loss of motor control. For example, higher operating temperatures than expected may cause the motor stator resistance to increase more than expected. Or battery state of charge decreasing more than expected may cause the DC link voltage to decrease more than expected, causing the motor stator voltage to decrease more than expected. And going out of range is not just a problem with slow changes in the motor parameters causing slow changes in the motor operating point. Rapid changes in the motor parameters can also cause the parameters to go out of range suddenly and temporarily, such as noise on the DC link voltage, for example. For this reason it has been found necessary to filter all the inputs to the feed-forward field weakening algorithm to limit their bandwidth to avoid having signals going out of range temporarily causing unstable operation. These filters slow down the dynamical response of the motor. And if these filters do not limit the parameter bandwidth enough, then unstable operation is still possible with a feed-forward approach.

Sudden changes in the sensed DC link voltage are particularly a problem for field weakening using a feed-forward technique because sudden changes in the sensed DC link voltage produce sudden changes in the motor speed, which determines which algorithm is used to perform field weakening. We have seen that there are three regions in the motor torque versus motor speed curve, and that field weakening is not needed in the lowest MTPA region below base speed, but depends on the both the motor current and motor voltage in the second region, and only on the motor voltage in the third MTPV region. This means that a different field weakening algorithm must be used in each of the three regions. It is therefore possible that a sudden change in the DC link voltage can cause the motor speed to suddenly change to a value that lies in a different region of the torque versus motor speed curve, causing a different field weakening algorithm to be selected. Ordinarily, this might happen only for small values of noise on the DC link voltage when the motor speed lies near a boundary between two different regions of the torque versus speed curve.

But if the DC link voltage is sampled while the power supply of the high voltage sensor is being lowered by a negative voltage spike, then a sudden drop in the sensed DC link voltage occurs which tricks the motor controller into believing that the DC link voltage has changed when in reality it has not changed. And because the motor speed is compensated for changes in the DC link voltage with SOC by multiplying the motor speed by the inverse of the DC link voltage, the motor controller will interpret a lower sensed DC link voltage as an increase in the motor speed. Therefore, if the motor was originally operating at a low speed in the first region of the torque versus speed curve where the motor torque is independent of the motor speed so no field

weakening is needed, after sensing that the DC link voltage has suddenly decreased, the motor controller will now believe that the motor speed is in the second region of the torque versus speed curve where field weakening must be applied. It therefore applies field weakening when field weakening is not needed because the true DC link voltage has not changed. This can result in the field weakening algorithm producing a value for the motor stator current that lies outside the range of operation of the PID controller for the motor stator current, which saturates the PID controller output and causes a loss of motor control. The result is sudden acceleration of the motor speed without the driver pressing on the accelerator pedal.

The conclusion is that both feed-forward and feedback field weakening algorithms are susceptible to unstable operation caused by a sudden decrease in the sensed DC link voltage caused by a negative voltage spike reducing the power supply of the high voltage sensor unless special care is taken to eliminate changes in the sensed DC link voltage during the analog-to-digital conversion process. One way to do this is by examining the sensed DC link voltage after digitization to see if it lies within a reasonable voltage range (e.g. equal to or greater than the minimum voltage associated with the minimum SOC value), and then either accepting the digitized output or re-sampling the sensor output if it does not lie in the reasonable range. This will avoid using a digitized value of the sensed DC link voltage that changes the region of operation under the torque versus motor speed curve.

References

1. Kim, D.-Y.; Lee, J.-H. "Low Cost Simple Look-Up Table-Based PMSM Drive Considering DC-Link Voltage Variation", *Energies* **2020**, 13, 3904. <https://www.mdpi.com/1996-1073/13/15/3904/pdf>
2. R. Cao, D. Hu and Y. Cao, "Practical Compensation Strategy for Accurate Torque Control in Mass-Produced High-speed Traction IPM E-Drives," *2021 IEEE Energy Conversion Congress and Exposition (ECCE)*, 2021, pp. 4654-4660. https://web.engr.oregonstate.edu/~caoy2/files/ECCE2021_RanCao.pdf
3. G. Pellegrino, E. Armando and P. Guglielmi, "Direct Flux Field-Oriented Control of IPM Drives With Variable DC Link in the Field-Weakening Region", in *IEEE Transactions on Industry Applications*, vol. 45, no. 5, pp. 1619-1627, Sept.-Oct. 2009. https://www.researchgate.net/publication/224562871_Direct_Flux_Field-Oriented_Control_of_IPM_Drives_With_Variable_DC_Link_in_the_Field-Weakening_Region
4. G. Pellegrino, R. I. Bojoi and P. Guglielmi, "Unified Direct-Flux Vector Control for AC Motor Drives," in *IEEE Transactions on Industry Applications*, vol. 47, no. 5, pp. 2093-2102, Sept.-Oct. 2011. <https://iris.polito.it/retrieve/handle/11583/2418739/54357/2010-IDC-408%20-%20Unified%20Direct-Flux%20Vector%20Control.pdf>
5. G. Pellegrino, E. Armando and P. Guglielmi, "Direct-Flux Vector Control of IPM Motor Drives in the Maximum Torque Per Voltage Speed Range," in *IEEE Transactions on Industrial Electronics*, vol. 59, no. 10, pp. 3780-3788, Oct. 2012. <https://iris.polito.it/retrieve/handle/11583/2460421/55146/Direct%20flux%20vector%20control%20of%20IPM%20motor%20drives.pdf>
6. Tianfu Sun, "Efficiency Optimised Control of Interior Permanent Magnet Synchronous Machine (IPMSM) Drives for Electric Vehicle Traction", Ph.D. Dissertation, University of Sheffield, Department of Electronic and Electrical Engineering, March 2016. https://etheses.whiterose.ac.uk/13610/1/Tianfu%20Sun_Efficiency%20Optimised%20Control%20of%20Interior%20Permanent%20Magnet%20Synchronous%20Machine%20%28IPMSM%29%20Drives%20for%20Electric%20Vehicle%20Traction.pdf
7. Jianjun Hu, Meixia Jia, Feng Xiao, Chunyun Fu, and Lingling Zheng, "Motor Vector Control Based on Speed-Torque-Current Map", *Applied Sciences*, 2020, 10(1), p. 78. <https://www.mdpi.com/2076-3417/10/1/78/pdf>
8. Group PED4-1038C, "Torque Control in Field Weakening Mode", Master's Thesis (Group Project), Institute of Energy Technology, Aalborg University, June 3, 2009. https://projekter.aau.dk/projekter/files/17643253/PED4_1038C.pdf
9. Dynamometer test results courtesy of Mountain Pass Performance located in Toronto, Canada.
10. E. Trancho et al., "IPMSM torque control strategies based on LUTs and VCT feedback for robust control under machine parameter variations," *IECON 2016 - 42nd Annual Conference of the IEEE Industrial Electronics Society*, 2016, pp. 2833-2838. <https://upcommons.upc.edu/bitstream/handle/2117/103294/final%20pdf.pdf>
11. Elena Trancho Olabbarri, "Field Weakening and Sensorless Control Solutions for Synchronous Machines Applied to Electric Vehicles", Ph.D. Dissertation, Universidad del Pais Vasco, February 26, 2018. <https://core.ac.uk/download/pdf/200970703.pdf>
12. E. Trancho et al., "PM-Assisted Synchronous Reluctance Machine Flux Weakening Control for EV and HEV Applications", *IEEE Transactions on Industrial Electronics*, 2018, Vol 65, pp. 2986-2995. http://dsp.tecnalia.com/bitstream/handle/11556/464/ALL_2rev-TIE-2017.pdf?sequence=1&isAllowed=y
13. NHTSA, DOT, *Event Data Recorders*, Final Regulatory Evaluation, Office of Regulatory Analysis and Evaluation National Center for Statistics and Analysis, July 2006. (Current EDR regulation active 2006 to present). <https://www.nhtsa.gov/sites/nhtsa.gov/files/fmvss/EDRFRIA.pdf>
14. NHTSA, DOT, *Event Data Recorders*, Notice of proposed rulemaking, 49 CFR Part 563 [Docket No. NHTSA-2022-0021], Federal Register, Vol. 87, No. 119, Wednesday, June 22, 2022. <https://www.govinfo.gov/content/pkg/FR-2022-06-22/pdf/2022-12860.pdf>
15. J. Jacob, S. Calligaro, O. Botessi and R. Petrella, "Design Criteria for Flux-Weakening Control Bandwidth and Voltage Margin in IPMSM Drives Considering Transient Conditions", *IEEE Transactions on Industry Applications*, June 6, 2021.

